Monthly Notices
of the
ROYAL ASTRONOMICAL SOCIETY

Mon. Not. R. Astron. Soc. **412,** 1787–1803 (2011) doi:10.1111/j.1365-2966.2010.18016.x

# Physical parameters of 62 eclipsing binary stars using the All Sky Automated Survey-3 data – I

Sukanta Deb★ and Harinder P. Singh

*Department of Physics & Astrophysics, University of Delhi, Delhi 110007, India*

Accepted 2010 November 10. Received 2010 November 9; in original form 2010 May 25

**ABSTRACT**

We present a detailed light-curve analysis of publicly available *V*-band observations of 62 binary stars, mostly contact binaries, obtained by the All Sky Automated Survey (ASAS)-3 project between 2000 and 2009. Eclipsing binaries are important astronomical targets for determining the physical parameters of component stars from the geometry of their orbits. They provide an independent direct method of measuring the radii of stars. We improved the ASAS determined periods and ephemerides, and obtained the Fourier parameters from the phased light curves of these 62 stars. These Fourier parameters were used for preliminary classification of the stars in our sample. The phased light curves were then analysed with the aid of the Wilson–Devinney light-curve modelling technique in order to obtain various geometrical and physical parameters of these binaries. The spectroscopic mass ratios as determined from the radial velocity measurements available in the literature were used as one of the inputs to the light-curve modelling. Thus reliable estimations of parameters of these binaries were obtained with combined photometric and spectroscopic data, and error estimates were made using the heuristic scan method. For several systems in the sample, the solutions were obtained for the first time and would serve as a good source in the future for light-curve analysis based on more precise follow-up CCD photometric observations. Out of 62 stars in the sample, photometric analysis of 39 stars is presented here for the first time using the ASAS photometry and precise spectroscopic mass ratios. From the analysis, we found 54 contact binaries, six semidetached binaries and two detached binaries. The Fourier parameters in the $a_2$–$a_4$ plane were used for preliminary classification, and the final classification was done based on the Roche lobe geometry obtained from the light-curve modelling.

**Key words:** binaries: close – binaries: eclipsing – stars: evolution – stars: fundamental parameters – stars: magnetic field – starspots.

## 1 INTRODUCTION

Eclipsing binaries are an important astrophysical tool for studying star formation and stellar structure, testing the theories of stellar evolution and determining the physical properties of stars. They have been used as standard candles (Paczynski 1997) to determine the size and structure of the Galaxy, as well as to constrain the cosmological distance ladder (Bonanos et al. 2006). They are potential targets since the orbital motion, inferred from the radial velocity curves and the shape of eclipses from the photometric light curves, can be entirely explained by the gravitation laws and geometry of the system. They are also useful for distance determinations since the radii and temperatures of the components can be reliably determined from the combined photometry and spectroscopy (Vilardell et al. 2010).

Contact binaries, also known as the W UMa stars, are low-mass eclipsing binaries consisting of ellipsoidal components with orbital periods less than 1 d, usually in the range $0.2 < P < 0.8$ d, with continuously changing brightness (Kang et al. 2002; Percy 2007). They consist of solar-type main-sequence components which fill their Roche lobes and share a common outer envelope at the inner Lagrangian point. The maxima of the light curves are rounded as the shapes of the two stars are strongly tidally distorted because of their proximity to one another (Shu 1982). Most of the W UMa type binaries have temperatures of the components roughly equal because of sharing a common envelope with the same entropy, thereby making the effective temperatures almost equal over the surfaces (Paczyński et al. 2006). There is also a subclass of contact binaries with temperature difference of 1000 K or larger between the components. Csizmadia & Klagyivik (2004) called these B-type contact binaries. In this paper, we follow the definition of B-type contact binaries as given by Csizmadia & Klagyivik (2004). B-type contact binaries are

★E-mail: sdeb@physics.du.ac.in; sukantodeb@gmail.com

sometimes called 'poor thermal contact binaries' (Rucinski & Duerbeck 1997).

The All Sky Automated Survey (ASAS) project started in 1997 with the goal of photometrically monitoring millions of stars brighter than 14 mag in the $V$ band and distributed all over the sky (Pojmanski 1997, 2002). The ASAS-3 system is located at Las Campanas Observatory and has been operating since 2000 August. It is equipped with 200/2.8 Minolta telephoto lenses and covers 8.8 $\times$ 8.8 deg$^2$ of the sky through the standard $V$ and $I$ filters. So far, ASAS has discovered more than 50 000 variables located south of declination $+28^\circ$ and nearly 10 000, among these newly identified variables, are eclipsing binaries. For more details about the ASAS project and the instruments, we refer the reader to Pojmanski (1997, 1998, 2002). These newly discovered binaries, among the others, are very valuable and their determination of absolute physical parameters will help to address several key problems related to stellar astrophysics.

The ASAS data base has time series photometric measurements of a large number of eclipsing binary stars. The light curves of these stars can provide reliable information about various parameters, once the mass ratios from the radial velocity measurements are available. The evolution of stars with cool convective envelopes, notably, of binary stars, is greatly affected by the dynamo-driven mass loss, magnetic braking and tidal friction which cause angular momentum loss from the orbit (Parihar et al. 2009). Therefore, enriching the total sample of new eclipsing binary stars with their parameters preliminarily determined from data bases like ASAS and their future follow-up regular observation using more precise CCD photometric data and spectroscopic radial velocity measurements will enhance our knowledge in understanding the nature, structure and evolution of binary stars.

Recently, the ASAS photometric data base has been used by Hełminiak et al. (2009) to determine the absolute and physical parameters for a sample of 18 detached binaries using the spectroscopic values of mass ratio $q_{\rm sp}$ obtained from their new radial velocity measurements. Out of 18 eclipsing binaries in their sample, 15 are new, discovered by ASAS.

The main rationale of this paper is to exploit the available ASAS photometric data of 62 binary stars which have complementary well-defined radial velocity measurements in the literature in order to determine their geometrical and physical parameters. In Section 2, we describe the criteria to select the sample in our present study. In Section 3, we describe a method to improve the period as determined by ASAS. Section 4 deals with the determination of Fourier parameters from the phased light curves and classification using the Fourier coefficients in the $a_2$–$a_4$ plane. In Section 5, we describe the light-curve analysis using the WD light-curve modelling technique to estimate the various geometrical and physical parameters of the 62 ASAS stars. In Section 6, we present results obtained from the light-curve modelling and compare to those in the literature, wherever available. Section 7 describes various relations for contact binaries. Finally, in Section 8, we present a summary and conclusions of this study.

## 2 SAMPLE SELECTION CRITERIA

### 2.1 The data

The number of photometric light curves of eclipsing binary stars has surpassed their spectroscopic radial velocity measurements with the advent of various all sky automated photometric surveys. Rucinski and collaborators (hereafter RC: Lu & Rucinski 1999; Rucinski & Lu 1999; Rucinski, Lu & Mochnacki 2000; Lu, Rucinski & Ogłoza 2001; Rucinski et al. 2001, 2002; Rucinski 2002; Rucinski et al. 2003; Pych et al. 2004; Rucinski et al. 2005; Pribulla et al. 2006; Rucinski & Duerbeck 2006; Duerbeck & Rucinski 2007; Pribulla et al. 2007; Rucinski et al. 2008; Pribulla et al. 2009a,b) started a project to obtain precise radial velocity measurements of a large number of binary stars. In practice, physical parameters of eclipsing binary stars are derived from photometric light-curve modelling which, in general, requires an accurate and precise mass ratio as an input obtained from the spectroscopic radial velocity measurements.

We searched for eclipsing binaries from the ASAS online data base which have well-defined determinations of mass ratios available from radial velocity measurements obtained by RC. We found 67 stars in the ASAS data base corresponding to the coordinates of identifiers of stars in RC's sample using the SIMBAD data base. However, light curves of the five ASAS stars turned out to be very noisy after they were phased with their respective periods as given in the data base. The light curves of these stars could not even be improved using the period determination technique as described in Section 3. Therefore, these stars were rejected for further analysis. These stars were 002524−4655.5 (BQ Phe), 050702−0047.6 (V1363 Ori), 124015−1848.0 (SX Crv), 131223+0239.3 (KZ Vir) and 164824+1708.1 (V918 Her). Our final sample thus consisted of 62 eclipsing binary stars. Light curves of each of the 62 stars were then examined carefully and outliers were removed after visual inspection. All the selected targets have evenly covered $V$-band light curves with an internal accuracy $\sim$0.03–0.11 mag having numbers of data points between 96 (062605+2759.9) and 1221 (204628−7157.0). The data for these 62 eclipsing binary stars, mostly contact binaries from the ASAS-3 data base, along with their spectroscopically determined mass ratios are used to model the light curves in order to obtain their various geometrical and physical parameters. The parameters determined for these 62 stars in this work, in turn, can be used as inputs to the analysis of more accurate and precise light curves based on follow-up observations. All the systems have their ASAS photometry available online.[1] On average, the number of observations per star is of the order of several hundred in the ASAS data base. These stars have a good phase coverage of their light curves.

### 2.2 Radial velocity and its importance

It is a widely accepted fact that physical parameters of binary stars obtained from photometric light-curve modelling are reliable only when the spectroscopically determined mass ratio is used as an input in the photometric light-curve modelling and kept fixed. In the light-curve modelling of binary stars, mass ratio is the most important parameter and should be obtained from precise spectroscopic radial velocity measurements. It plays an important role in deriving the accurate masses and radii of the components, which are the key parameters in understanding the structure and evolution of binary stars. It has been seen from the literature that determination of mass ratio from the photometric light-curve modelling is exceedingly difficult. For a partially eclipsing binary, it is impossible to reliably measure the mass ratio from the photometric modelling even with highly accurate photometric data. On the other hand, the mass ratios determined from the photometric data may be reliable only for a total-eclipse configuration of the binary systems, as such light curves show characteristic inner contacts with duration of

[1] http://www.astrouw.edu.pl/asas

totality setting a strong constraint on the $(q, i)$ pair (Rucinski 2001). The literature is crowded with physical parameter estimations using the photometric mass ratio ($q_{\rm ph}$) obtained from the light-curve modelling for many partially eclipsing systems which were later modified when subsequent radial velocities became available.

## 3 UPDATING THE ASAS PERIOD

The automated surveys like ASAS offer a unique opportunity to study the properties of a large number of stars. However, the processing of the huge amount of data in these data bases is quite challenging, even when looking at seemingly small issues such as period determination and classification (Derekas, Kiss & Bedding 2007). Although the periods determined for most of the stars in the ASAS data base are reasonably accurate (except 185318+2113.5), we have found that the ASAS periods need to be updated to the improved quality of data available at present. Periods of variable stars in the ASAS data base were in general determined very well during the preparation of the catalogue. However, the data for some parts of the sky were analysed many years ago, when the time-span was much shorter. Therefore, the accuracy was not good as can be obtained today.

It has been found that the period determination can be further improved by the use of methods such as string lengths (Derekas et al. 2007) or the minimization of entropy method (Deb et al. 2009). The new period determinations result in the improvement of the ASAS periods to the fifth or sixth decimal place. This period improvement has resulted in revealing the accurate shapes of the phased light curves of the ASAS eclipsing binaries. In practice, when the period is accurate enough, the phased data are clearly arranged with minimum scatter due to noise. On the other hand, when the light curve is folded into phase by an incorrect period, the data get randomized and more scattered.

We have used the minimization of entropy (hereafter, ME) method to improve and update the period as determined by ASAS, which is based on the minimization of the information entropy of the light curve (Cincotta, Mendez & Nunez 1995). It is based on the fact that the light curves in the phase–magnitude $(\Phi, x)$ space are more ordered when the phases are determined using the correct period, where phase $\Phi$ is defined as

$$\Phi = \frac{(t - t_0)}{P} - \mathrm{Int}\left[\frac{(t - t_0)}{P}\right], \quad (1)$$

where $t_0$ is the initial epoch of the variable star light curve and $t$ is the time of observations. The value of $\Phi$ is from 0 to 1, corresponding to a full cycle of the orbital period $P$.Int denotes the integer part of the quantity. The light-curve data $(t_i, x_i)$ are phased into the phase–magnitude space according to the trial period. Now the phase–magnitude space is divided into $n \times m$ bins. Let $\mu_{ij}$ be the number of observations in the $(i, j)$ bin normalized by the total number of data, then the entropy $S$ is

$$S = \sum_{i=1}^{n} \sum_{j=1}^{m} \mu_{ij} \ln(\mu_{ij}), \quad (2)$$

for all $\mu_{ij} > 0$. If the trial period is not the true one, the light-curve points will be distributed uniformly in the $(\Phi, x)$ plane and the entropy will be maximum. On the other hand, if the trial period matches with the actual period, the points will be limited into a small region of the plane and the entropy will then be minimum, which will correspond to the best period of the light curve. In our case, we applied the ME method around $\pm 1$ per cent of the ASAS-determined periods. An example of the period improvement is shown in Fig. 1.

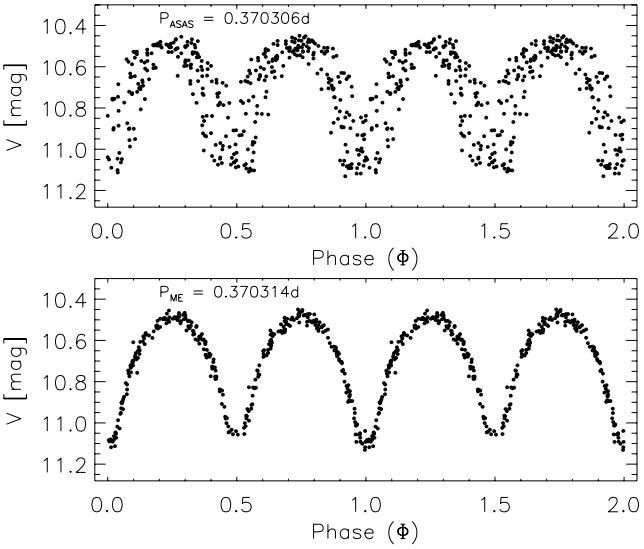


**Figure 1.** The upper panel shows the phased light curve for the star ASAS 193524+0550.3 with the original ASAS period $P_{\rm ASAS} = 0.370\,306$ d. The lower panel shows the phased light curve of the same star with the improved period determined in the present work, $P_{\rm ME} = 0.370\,314$ d.

The typical improvement results in a change in the fifth or sixth decimal place. For 185318+2113.5, we have found that the ASAS period is not correct, as no significant periodicity can be confirmed from the phased light curve with $P_{\rm ASAS} = 21.846\,85$ d. For preliminary period determination of this star only, we have used the phase dispersion minimization method (hereafter PDM; Stellingwerf 1978). In Fig. 2, we show the PDM results applied to the light curve of ASAS 185318+2113.5. The three dominant peaks of the PDM results are 0.493 326, 0.246 658 and 0.395 712 d in increasing $\Theta$ values, where $\Theta$ is defined as in Stellingwerf (1978). We also tried to improve the most dominant period 0.493326 d, using the ME method. The ME method is run around $\pm 1$ per cent of the period 0.493326 d. The period is found to be $P_{\rm ME} = 0.493\,322$ d. In this case, the periods determined by both PDM and ME methods are nearly identical. The light curves of ASAS 185318+2113.5 phased

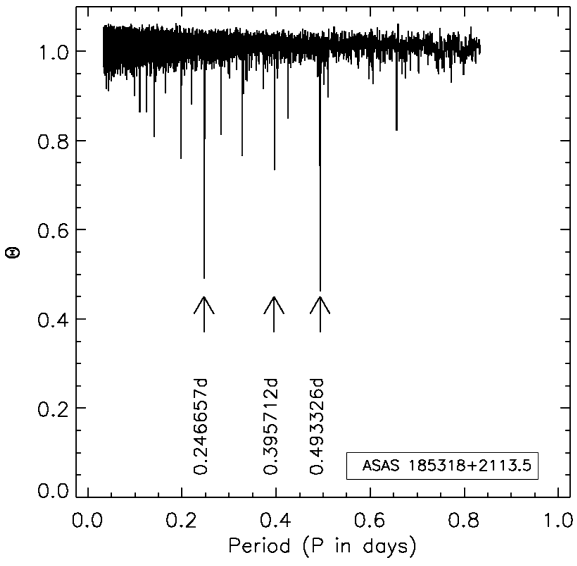


**Figure 2.** Plot of $\Theta$ versus period for ASAS 185318+2113.5 as determined from the PDM.

**Table 1.** Basic information on the ASAS stars used for the analysis.

| Serial No. | ASAS ID | Other ID | $\alpha$(2000) | $\delta$(2000) | $P_{\rm ASAS}$ (d) | $P_{\rm ME}$ (d) | Type | $V$ (mag) | $J-K$ (mag) | Epoch(PHOEBE) (JD −245 0000) |
|---|---|---|---|---|---|---|---|---|---|---|
| 1 | 003628+2132.3 | DZ Psc | 00 36 27.95 | +21 32 14.63 | 0.366 125 | 0.366 131 | A | 11.126 | 0.253(35) | 2970.55578 (53) |
| 2 | 011638−3942.S | AD Phe | 01 16 38.07 | −39 42 31.32 | 0.379 92 | 0.379 919 | W | 10.290 | 0.400(33) | 1903.57977 (27) |
| 3 | 012104+0736.3 | AQ Psc | 01 21 03.56 | +07 36 21.63 | 0.475 611 | 0.475 604 | A | 8.67 | 0.255(30) | 3653.71572 (47) |
| 4 | 014656−0945.1 | TT Cet | 01 46 56.50 | −09 45 09.74 | 0.485 96 | 0.485 952 | B | 10.9 | 0.250(29) | 5103.86538 (27) |
| 5 | 014854−2053.6 | TW Cet | 01 48 54.14 | −20 53 34.60 | 0.316 849 | 0.316 851 | A | 10.7 | 0.492(38) | 4476.61915 (09) |
| 6 | 023833−1417.9 | DY Cet | 02 38 33.18 | −14 17 56.73 | 0.440 790 | 0.440 790 | A | 9.8 | 0.258(34) | 3644.73338 (18) |
| 7 | 024952+0856.3 | EE Cet | 02 49 52.26 | +08 56 17.95 | 0.379 92 | 0.379 925 | W | 9.6 | 0.280(47) | 2643.59790 (42) |
| 8 | 030701−5608.1 | SZ Hor | 03 07 01.23 | −56 08 04.45 | 0.625 11 | 0.625 102 | B | 11.214 | 0.217(31) | 4314.85995 (21) |
| 9 | 030953−0653.6 | UX Eri | 03 09 52.74 | −06 53 33.56 | 0.445 28 | 0.445 289 | W | 10.639 | 0.374(33) | 2954.68085 (31) |
| 10 | 033459+1742.6 | V1123 Tau | 03 34 58.54 | +17 42 38.04 | 0.399 946 | 0.399 947 | W | 9.97 | 0.246(50) | 2621.65355 (28) |
| 11 | 034814+2218.9 | EQ Tau | 03 48 13.43 | +22 18 50.92 | 0.341 347 | 0.341 350 | A | 11.196 | 0.376(28) | 4846.56948 (27) |
| 12 | 034928+1254.7 | V1128 Tau | 03 49 27.77 | +12 54 43.84 | 0.305 372 | 0.305 371 | W | 9.353 | 0.454(30) | 3751.55994 (13) |
| 13 | 035153−1031.8 | BV Eri | 03 51 53.34 | −10 31 49.46 | 0.507 654 | 0.507 655 | B | 8.32 | 0.221(33) | 4300.91807 (25) |
| 14 | 041209−1028.2 | YY Eri | 04 12 08.85 | −10 28 09.96 | 0.321 499 | 0.321 498 | W | 8.41 | 0.443(34) | 3454.51428 (15) |
| 15 | 042925−3334.6 | CT Eri | 04 29 24.79 | −33 34 34.33 | 0.634 19 | 0.634 196 | B | 10.22 | 0.215(36) | 5113.80003 (36) |
| 16 | 051114−0833.4 | ER Ori | 05 11 14.50 | −08 33 24.66 | 0.4234 | 0.423 406 | W | 10.00 | 0.317(31) | 1967.52334 (27) |
| 17 | 051832−6813.6 | RW Dor | 05 18 32.54 | −68 13 32.76 | 0.285 461 | 0.285 463 | W | 10.80 | 0.573(33) | 3466.52582 (11) |
| 18 | 062605+2759.9 | AH Aur | 06 26 04.93 | +27 59 56.40 | 0.247 053 | 0.494 106 | A | 10.176 | 0.329(28) | 2970.77551 (66) |
| 19 | 064558−0017.5 | DD Mon | 06 45 57.83 | −00 17 31.90 | 0.568 03 | 0.568 019 | ESD | 11.1 | 0.388(35) | 3051.71881 (22) |
| 20 | 071058−0352.8 | V753 Mon | 07 10 57.85 | −03 52 43.19 | 0.677 05 | 0.677 045 | ESD | 8.34 | 0.203(32) | 2701.61458 (17) |
| 21 | 073246−2047.5 | TY Pup | 07 32 46.23 | −20 47 31.07 | 0.819 25 | 0.819 243 | A | 8.62 | 0.257(61) | 1876.71203 (25) |
| 22 | 073338−5007.4 | HI Pup | 07 33 38.21 | −50 07 25.05 | 0.432 618 | 0.432 618 | A | 10.70 | 0.349(30) | 1924.65641 (40) |
| 23 | 073905−0239.1 | V868 Mon | 07 39 04.83 | −02 39 05.54 | 0.637 704 | 0.637 704 | A | 8.9 | 0.160(33) | 3745.74415 (63) |
| 24 | 084002+1900.0 | TX Cnc | 08 40 01.71 | +18 59 59.51 | 0.382 882 | 0.382 883 | W | 10.026 | 0.355(27) | 4409.86025 (45) |
| 25 | 084108−3212.1 | TZ Pyx | 08 41 08.26 | −32 12 03.02 | 2.318 500 | 2.318 530 | ED | 10.67 | 0.083(33) | 3805.69203 (51) |
| 26 | 100141+1724.5 | XY Leo | 10 01 40.43 | +17 24 32.70 | 0.284 098 | 0.284 101 | W | 9.67 | 0.701(41) | 2733.60886 (28) |
| 27 | 100234+1702.8 | XZ Leo | 10 02 34.19 | +17 02 47.14 | 0.487 736 | 0.487 736 | A | 10.29 | 0.171(30) | 3339.81755 (30) |
| 28 | 100248+0105.7 | Y Sex | 10 02 47.96 | +01 05 40.35 | 0.419 82 | 0.487 736 | A | 9.97 | 0.278(32) | 4589.56507 (21) |
| 29 | 101602−0618.5 | XX Sex | 10 02 47.96 | +01 05 40.35 | 0.540 111 | 0.540 108 | A | 9.32 | 0.243(38) | 4164.67735 (40) |
| 30 | 104033+1334.0 | UZ Leo | 10 40 33.19 | +13 34 00.86 | 0.618 06 | 0.618 057 | A | 9.75 | 0.208(30) | 3809.71938 (26) |
| 31 | 105030−0241.7 | VY Sex | 10 50 29.72 | −02 41 43.05 | 0.443 432 | 0.443 433 | W | 9.01 | 0.346(38) | 4918.59063 (21) |
| 32 | 110211+0953.7 | AM Leo | 11 02 10.89 | +09 53 42.69 | 0.365 798 | 0.365 799 | W | 9.31 | 0.328(30) | 3739.83590 (20) |
| 33 | 110505+0509.1 | AP Leo | 11 05 05.02 | +05 09 06.42 | 0.430 356 | 0.430 358 | A | 9.53 | 0.368(33) | 4656.47341 (33) |
| 34 | 120103+1300.5 | AG Vir | 12 01 03.50 | +13 00 30.02 | 0.642 65 | 0.642 648 | A | 8.52 | 0.145(32) | 3190.49382 (47) |
| 35 | 121206+2232.0 | CC Com | 12 12 06.20 | +22 31 58.00 | 0.220 686 | 0.220 686 | W | 11.00 | 0.741(26) | 3012.86701 (16) |
| 36 | 123300+2642.9 | RW Com | 12 33 00.28 | +26 42 58.38 | 0.237 348 | 0.237 346 | W | 11.00 | 0.618(34) | 4918.69817 (20) |
| 37 | 131032−0409.5 | PY Vir | 13 10 32.22 | −04 09 32.59 | 0.311 251 | 0.311 248 | ESD | 9.60 | 0.572(38) | 5002.63460 (25) |
| 38 | 134607+0506.9 | HT Vir | 13 46 06.75 | +05 06 56.27 | 0.407 672 | 0.407 672 | ESD | 7.16 | 0.324(30) | 4919.78943 (20) |
| 39 | 141726+1234.1 | VW boo | 14 17 26.03 | +12 34 03.45 | 0.342 315 | 0.342 315 | A | 10.539 | 0.467(29) | 2840.61055 (20) |
| 40 | 141937+0553.8 | NN Vir | 14 19 37.74 | +05 53 46.66 | 0.480 687 | 0.480 688 | A | 7.64 | 0.240(37) | 3576.56349 (36) |
| 41 | 143504+0906.8 | CK Boo | 14 35 03.76 | +09 06 49.39 | 0.355 154 | 0.355 152 | A | 9.09 | 0.295(44) | 2670.85694 (29) |
| 42 | 144803+1356.7 | EL Boo | 14 48 03.40 | +13 56 41.19 | 0.413 767 | 0.413 766 | ESD | 9.35 | 0.282(34) | 4633.62612 (64) |
| 43 | 152243+1615.7 | OU Ser | 15 22 43.47 | +16 15 40.74 | 0.148 382 | 0.296 768 | A | 8.25 | 0.376(31) | 4891.85851 (51) |
| 44 | 153152−1541.1 | VZ Lib | 15 31 51.76 | −15 41 10.19 | 0.358 259 | 0.358 256 | A | 10.341 | 0.379(35) | 4487.87049 (22) |
| 45 | 155649+2216.0 | AU Ser | 15 56 49.40 | +22 16 01.00 | 0.386 498 | 0.386 498 | A | 10.50 | 0.509(28) | 4299.48460 (29) |
| 46 | 164121+0030.4 | V502 Oph | 16 41 20.86 | +00 30 27.37 | 0.453 39 | 0.453 388 | W | 8.53 | 0.345(29) | 4701.54638 (29) |
| 47 | 165717+1059.8 | V2357 Oph | 16 57 16.76 | +10 59 51.38 | 0.207 783 | 0.415 568 | A | 10.52 | 0.426(31) | 4691.58664 (93) |
| 48 | 171358+1621.0 | AK Her | 17 13 57.82 | +16 21 00.61 | 0.421 522 | 0.421 524 | A | 8.51 | 0.313(34) | 5071.56284 (24) |
| 49 | 173356+0810.0 | V2377 Oph | 17 33 56.05 | +08 09 57.81 | 0.425 403 | 0.425 406 | W | 8.56 | 0.333(34) | 3652.51616 (66) |
| 50 | 175332−0354.9 | V2610 Oph | 17 53 32.26 | −03 54 55.33 | 0.426 52 | 0.426 514 | ESD | 9.20 | 0.393(34) | 2508.56147 (42) |
| 51 | 180921+0909.1 | V839 Oph | 18 09 21.27 | +09 09 03.63 | 0.409 | 0.409 008 | A | 8.984 | 0.344(28) | 3547.70415 (15) |
| 52 | 182913+0647.3 | V2612 Oph | 18 29 13.01 | +06 47 13.72 | 0.3753 | 0.375 309 | W | 9.44 | 0.279(38) | 4234.79999 (40) |
| 53 | 185318+2113.5 | V1003 Her | 18 53 17.54 | +21 13 32.74 | 21.846 85 | 0.493 322 | B | 9.795 | 0.234(32) | 4286.34912 (96) |
| 54 | 193524+0550.3 | V417 Aql | 19 35 24.12 | +05 50 17.66 | 0.370 306 | 0.370 314 | W | 10.647 | 0.354(33) | 4216.88855 (13) |
| 55 | 194813+0918.5 | OO Aql | 19 48 12.65 | +09 18 32.38 | 0.506 786 | 0.506 794 | A | 9.51 | 0.440(36) | 5070.71740 (18) |
| 56 | 203113+0513.2 | MR Del | 20 31 13.47 | +05 13 08.50 | 0.521 69 | 0.521 692 | ED | 11.01 | 0.624(28) | 4742.53659 (35) |
| 57 | 204628−7157.0 | MW Pav | 20 46 27.76 | −71 56 58.48 | 0.795 | 0.794 994 | A | 8.80 | 0.229(30) | 1887.52447 (26) |
| 58 | 205710+1939.0 | LS Del | 20 57 10.29 | +19 38 59.22 | 0.363 84 | 0.363 842 | W | 8.654 | 0.308(37) | 4628.82082 (97) |
| 59 | 222257+1619.4 | BB Peg | 22 22 56.89 | +16 19 27.84 | 0.361 487 | 0.361 502 | W | 10.967 | 0.388(28) | 3586.70575 (18) |
| 60 | 233655+1548.1 | V407 Peg | 23 36 55.37 | +15 48 06.43 | 0.636 88 | 0.636 882 | A | 9.28 | 0.181(33) | 5084.69145 (51) |
| 61 | 234535+2528.3 | V357 Peg | 23 45 35.06 | +25 28 18.94 | 0.578 45 | 0.578 450 | A | 9.06 | 0.178(34) | 4693.78588 (34) |
| 62 | 234718−0805.2 | EL Aqr | 23 47 18.35 | −08 05 12.09 | 0.481 41 | 0.481 412 | A | 10.572 | 0.249(35) | 4456.57279 (35) |

**Table 2.** Spectral type and radial velocity information for the ASAS stars.

| ASAS ID | Spectral type | $K_1$ (km s$^{-1}$) | $\sigma K_1$ (km s$^{-1}$) | $K_2$ (km s$^{-1}$) | $\sigma K_2$ (km s$^{-1}$) | Mass ratio ($q$) | References |
|---|---|---|---|---|---|---|---|
| 003628+2132.3 | F7V | 40.39 | 2.64 | 297.98 | 4.18 | 0.136(10) | 7 |
| 011638−3942.S | F9/G0V | 89.04 | 3.10 | 242.41 | 1.42 | 0.370(10) | 11 |
| 012104+0736.3 | F5/8V | 59.50 | 0.40 | 263.30 | 1.90 | 0.226(02) | 1, 13 |
| 014656−0945.1 | F4V | 107.90 | 10.30 | 276.00 | 27.00 | 0.39(07) | 11 |
| 014854−2053.6 | G1V | 157.40 | 3.26 | 209.66 | 3.84 | 0.75(03) | 11 |
| 023833−1417.9 | F5V | 90.84 | 2.11 | 255.40 | 2.28 | 0.356(9) | 13 |
| 024952+0856.3 | F8V | 84.05 | 1.24 | 266.92 | 1.54 | 0.315(5) | 6 |
| 030701−5608.1 | F3V | 109.51 | 6.60 | 231.34 | 13.50 | 0.47(04) | 11 |
| 030953−0653.6 | F9V | 91.75 | 1.55 | 245.76 | 1.86 | 0.373(21) | 11 |
| 033459+1742.6 | G0V | 71.08 | 0.84 | 254.71 | 0.84 | 0.279(4) | 12 |
| 034814+2218.9 | G2V | 112.41 | 1.43 | 254.38 | 2.42 | 0.442(7) | 4 |
| 034928+1254.7 | F8V | 130.48 | 1.27 | 244.19 | 1.28 | 0.534(6) | 12 |
| 035153−1031.8 | F3/4V | 65.71 | 2.90 | 221.10 | 9.90 | 0.30(02) | 11 |
| 041209−1028.2 | G3V | 107.30 | 2.27 | 242.57 | 2.56 | 0.401 | 11 |
| 042925−3334.6 | F2/3V | 68.30 | 14.90 | 229.10 | 48.00 | 0.30(09) | 11 |
| 051114−0833.4 | F7/8V | 147.98 | 2.30 | 225.48 | 2.35 | 0.656(12) | 13 |
| 051832−6813.6 | G4/5V | 134.35 | 3.46 | 213.06 | 4.65 | 0.63(03) | 11 |
| 062605+2759.9 | F7V | 47.20 | 1.16 | 279.61 | 2.80 | 0.169(59) | 1 |
| 064558−0017.5 | G0V | 133.32 | 3.06 | 198.85 | 3.18 | 0.670(19) | 13 |
| 071058−0352.8 | A8V | 176.07 | 0.97 | 170.76 | 0.97 | 1.031(9) | 3 |
| 073246−2047.5 | F3V | 55.68 | 5.52 | 226.80 | 15.40 | 0.25(03) | 11 |
| 073338−5007.4 | F6V | 50.20 | 15.40 | 265.20 | 17.20 | 0.19(06) | 11 |
| 073905−0239.1 | F2V | 91.21 | 1.83 | 244.67 | 2.22 | 0.373(8) | 13 |
| 084002+1900.0 | F8V | 100.77 | 0.82 | 221.67 | 0.91 | 0.455(11) | 9 |
| 084108−3212.1 | A8/9V | 126.22 | 2.09 | 130.79 | 1.52 | 0.965(20) | 11 |
| 100141+1724.5 | K0V | 144.65 | 1.10 | 198.41 | 1.11 | 0.729(7) | 10 |
| 100234+1702.8 | A8/F0V | 262.55 | 2.60 | 91.49 | 1.80 | 0.348(29) | 2 |
| 100248+0105.7 | F5/6V | 54.96 | 2.30 | 281.94 | 2.86 | 0.195(8) | 13 |
| 101602−0618.5 | F3V | 25.80 | 0.45 | 258.51 | 1.54 | 0.100(2) | 10 |
| 104033+1334.0 | A9/F1V | 79.69 | 1.12 | 262.87 | 1.89 | 0.303(24) | 2 |
| 105030−0241.7 | F9.5 | 74.33 | 0.91 | 237.30 | 1.32 | 0.313(5) | 7 |
| 110211+0953.7 | F5V | 115.56 | 0.97 | 251.98 | 1.17 | 0.459(4) | 10 |
| 110505+0509.1 | F8V | 78.20 | 2.30 | 263.10 | 2.90 | 0.297(09) | 1 |
| 120103+1300.5 | A5V | 93.39 | 1.06 | 244.24 | 1.97 | 0.382(21) | 9 |
| 121206+2232.0 | K4/5V | 124.83 | 1.34 | 237.00 | 1.09 | 0.527(6) | 10 |
| 123300+2642.9 | K2/5V | 112.04 | 1.28 | 237.70 | 1.29 | 0.471(6) | 13 |
| 131032−0409.5 | K1/2V | 152.78 | 0.77 | 197.58 | 0.77 | 0.773(5) | 12 |
| 134607+0506.9 | F8V | 169.39 | 1.00 | 208.54 | 1.00 | 0.812(8) | 5 |
| 141726+1234.1 | G5V | 101.39 | 1.07 | 236.74 | 1.03 | 0.428(5) | 13 |
| 141937+0553.8 | F0/1V | 112.68 | 0.71 | 229.28 | 1.24 | 0.491(11) | 2 |
| 143504+0906.8 | F7/8V | 31.66 | 0.78 | 285.31 | 1.63 | 0.111(52) | 2 |
| 144803+1356.7 | F5V | 64.19 | 1.70 | 259.07 | 1.89 | 0.248(7) | 13 |
| 152243+1615.7 | F9/G0V | 40.59 | 0.59 | 234.24 | 0.69 | 0.173(17) | 3 |
| 153152−1541.1 | G0V | 84.10 | 3.84 | 252.20 | 4.55 | 0.33(4) | 5, 15 |
| 155649+2216.0 | G4V | 138.77 | 1.33 | 195.64 | 1.34 | 0.709(8) | 13 |
| 164121+0030.4 | G0V | 82.71 | 1.03 | 246.70 | 1.00 | 0.335(9) | 8 |
| 165717+1059.8 | G5V | 44.12 | 1.63 | 190.93 | 2.90 | 0.231(10) | 7 |
| 171358+1621.0 | F4V | 70.52 | 1.12 | 254.40 | 2.27 | 0.277(24) | 9 |
| 173356+0810.0 | G0/G1V | 159.64 | 0.70 | 62.99 | 0.62 | 0.395(12) | 5 |
| 175332−0354.9 | F8/G2V | 72.06 | 2.06 | 247.42 | 2.08 | 0.291(9) | 13 |
| 180921+0909.1 | F7V | 84.82 | 1.33 | 278.52 | 2.01 | 0.305(24) | 2 |
| 182913+0647.3 | F7V | 71.33 | 0.66 | 249.09 | 0.89 | 0.286(3) | 10 |
| 185318+2113.5 | A7 | 64.07 | 0.94 | 171.91 | 0.94 | 0.373(6) | 12 |
| 193524+0550.3 | F7V | 97.00 | 1.60 | 268.20 | 2.70 | 0.362(7) | 1, 13 |
| 194813+0918.5 | F9V | 153.03 | 0.93 | 180.81 | 1.14 | 0.846(7) | 10 |
| 203113+0513.2 | K2V | 135.74 | 1.27 | 148.32 | 1.27 | 0.915(12) | 13 |
| 204628−7157.0 | F3IV/V | 52.35 | 1.15 | 229.34 | 3.52 | 0.228(8) | 14 |
| 205710+1939.0 | F5/8V | 69.00 | 1.60 | 184.80 | 2.20 | 0.375(10) | 1, 13 |
| 222257+1619.4 | F7V | 97.20 | 1.50 | 270.20 | 2.50 | 0.360(06) | 1, 13 |
| 233655+1548.1 | F0V | 63.92 | 1.12 | 250.02 | 1.16 | 0.256(6) | 12 |
| 234535+2528.3 | F2V | 93.78 | 0.86 | 234.08 | 0.87 | 0.401(4) | 12 |
| 234718−0805.2 | F3V | 53.38 | 1.53 | 263.34 | 4.38 | 0.203(8) | 4 |

1. Lu & Rucinski (1999); 2. Rucinski & Lu (1999); 3. Rucinski et al. (2000); 4. Rucinski et al. (2001); 5. Lu et al. (2001); 6. Rucinski et al. (2002); 7. Rucinski et al. (2003); 8. Pych et al. (2004); 9. Pribulla et al. (2006); 10. Pribulla et al. (2007); 11. Duerbeck & Rucinski (2007); 12. Rucinski et al. (2008) ; 13. Pribulla et al. (2009b); 14. Rucinski & Duerbeck (2006); 15. Szalai et al. (2007).

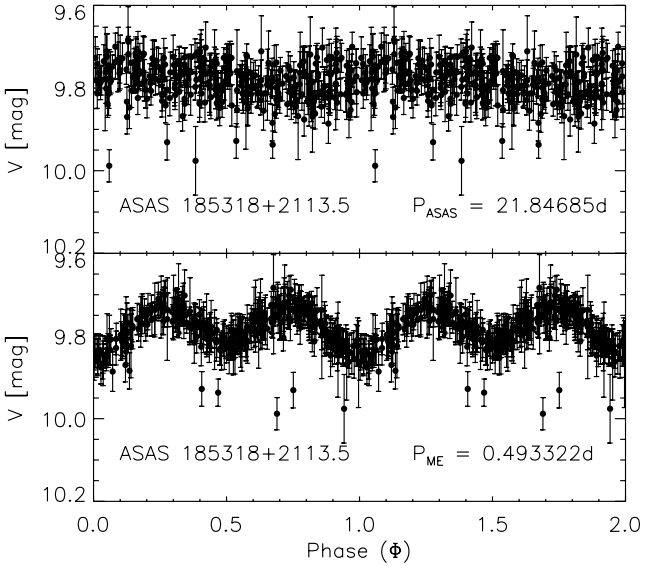


**Figure 3.** The upper panel shows the phased light curve of ASAS 185318+2113.5 determined from the ASAS period $P_{\rm ASAS} = 21.84685$ d. The lower panel shows the phased light curve of the same star with period $P_{\rm ME} = 0.493\,322$ d.

with the ASAS-determined period $P_{\rm ASAS}$ and our determined period $P_{\rm ME}$ are shown in Fig. 3. Our photometric analysis reveals that the star is at a very low inclination angle $i(^\circ) = 41.59 \pm 2.78$ and is a B-type contact binary with $\Delta T = 2316 \pm 647$ K. However, the low noisiness of the ASAS-3 data and its low amplitude make this star a good candidate for accurate follow-up observations. In Table 1, we list the serial numbers, ASAS identification names, SIMBAD identification names, J2000 coordinates, ASAS periods ($P_{\rm ASAS}$), updated periods determined using the ME method ($P_{\rm ME}$), type of binary determined from the light-curve analysis, $V$ band magnitudes, infrared $(J - K)$ colour indices (Cutri et al. 2003) and epochs of minimum light determined from the light-curve modelling. In Table 2, we list the spectral type, radial velocity semi-amplitudes of the components and their errors, mass ratios and references for the radial velocity measurements.

## 4 DETERMINATION OF FOURIER PARAMETERS AND CLASSIFICATION

Rucinski (1993) showed that the light curves of W UMa type systems can be quantitatively described by using only the two coefficients $a_2$ and $a_4$ of the cosine decomposition $\sum a_i \cos(2\pi i\Phi)$. The observed light curves were fitted with a Fourier series of the form:

$$m(\Phi) = m_0 + \sum_{i=1}^{4} [a_i \cos(2\pi i\Phi) + b_i \sin(2\pi i\Phi)], \quad (3)$$

where $m(\Phi)$ is the phased light curve, $m_0$ is the mean magnitude and the zero-point of the phased light curve corresponds to the primary minimum. Examples of the typical Fourier fits to the ASAS light curves are shown in Fig. 4. The Fourier parameters of the 62 binaries are listed in Table 3. The resulting distribution of the selected sample in the $a_2$–$a_4$ plane is shown in Fig. 5. The continuous envelope for separating the contact binaries from rest of the sample is shown by the relation $a_4 = a_2(0.125 + a_2)$. This is similar to the envelope relation $a_4 = a_2(0.125 - a_2)$ for negative $a_2$ and $a_4$ coefficients of Rucinski (1997b). This gives the envelope for the inner contact. The stars lying below this envelope are contact binaries, whereas those lying above it are semidetached and detached binaries. The stars lying on or above the envelope can be identified by the serial numbers 19, 20, 25, 38, 42, 50 and 56, respectively, corresponding to their ASAS IDs 064558−0017.5, 071058−0352.8, 084108−3212.1, 134607+0506.9, 144803+1356.7, 175332−0354.9 and 203113+0513.2, respectively. Out of these stars, we have identified two stars, 084108−3212.1 and 203113+0513.2, as detached binaries (ED) and the remaining stars as semidetached binaries (ESD) following the boundary lines of Derekas et al. (2007). In addition, the star with serial number 37 having ASAS ID 131032−0409.5 is found to be of ESD-type from the light-curve modelling although it lies slightly below the envelope. The stars having ASAS IDs 071058−0352.8 and 175332−0354.9 were also found to be of ESD-types by Zola et al. (2004) and Tas & Evren (2006), respectively. In general, the Fourier coefficient $a_2$ relates to the amplitude, $a_1$ and $a_3$ to the difference in the depth of the eclipses and $b_1$ to the difference between the two maxima (Paczyński et al. 2006; Rucinski 1997a). The phenomenon of difference in the height of the two maxima is called the O'Connell (1951) effect. In Fig. 6, we have plotted the temperature differences ($\Delta T$) obtained from the light-curve modelling versus $a_1 + a_3$ for the 62 eclipsing binaries in the present sample. The stars with serial numbers 4, 8, 13, 15, 19 and 53 were found to be binaries having temperature differences of 1000 K or larger between the components obtained from the light-curve modelling. However, sometimes the Fourier fit does not reproduce the bottom of the eclipses very well, and the algorithm misclassifies the objects. For example, the star having serial number 45 with ASAS ID 155649+2216.0 may be misclassified as a B-type system by the Fourier fitting algorithm because it gives higher value of $a_1$, although it is not a B-type binary having $\Delta T \sim 316$ K. The classification results of eclipsing binary stars based on the single-band photometry using the Fourier coefficients and without any spectroscopic information are generally considered preliminary (Paczyński et al. 2006). It should be noted that the star having serial number 53 with ASAS ID 185318+2113.5 is a B-type contact binary obtained from the light-curve modelling, although it has smaller values of the Fourier coefficients $a_1$ and $a_3$. We have also found that when the sum $(a_1 + a_3)$ is normalized by $a_2$, the star with serial number 53 moves right in Fig. 6. This implies that the coefficients $a_1$ and $a_3$ are obviously inclination-dependent and also, to some extent, on amplitude. It is obvious that the Fourier method has given smaller values of $(a_1 + a_3)$ for this very low inclination star. More accurate morphological classification of eclipsing binary stars is usually done from the photometric light-curve modelling with the mass ratio $q$ obtained from spectroscopic radial velocity measurements.

## 5 LIGHT-CURVE MODELLING

The mass ratios obtained from radial velocity measurements, mostly by RC, were used with the ASAS photometry to derive the geometrical and physical parameters of the 62 binary stars. For the light-curve modelling, we have used the WD code (Wilson & Devinney 1971; Wilson 1979, 1990) as implemented in the software PHOEBE (Prša & Zwitter 2005). In the WD code, some of the parameters need to be fixed and the convergence of the solutions was obtained using the methods of multiple-subsets. In the code, since most of the binaries were the contact binaries,the mode 3 version was the most suitable for the light-curve analysis. However, at the outset, mode 2 (detached) was used to get the convergence of the solution and then rapidly ran into mode 3 for the final convergence. In the light-curve analysis using the WD code, star 1 is the one eclipsed at

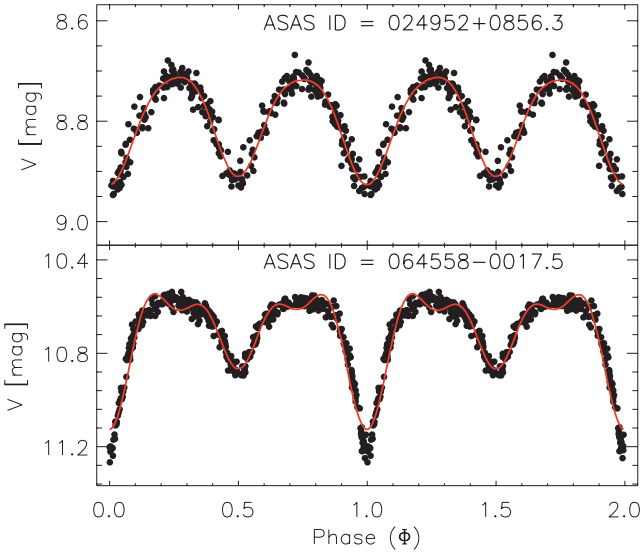


**Figure 4.** Typical Fourier fits for the ASAS eclipsing binaries used for the analysis.

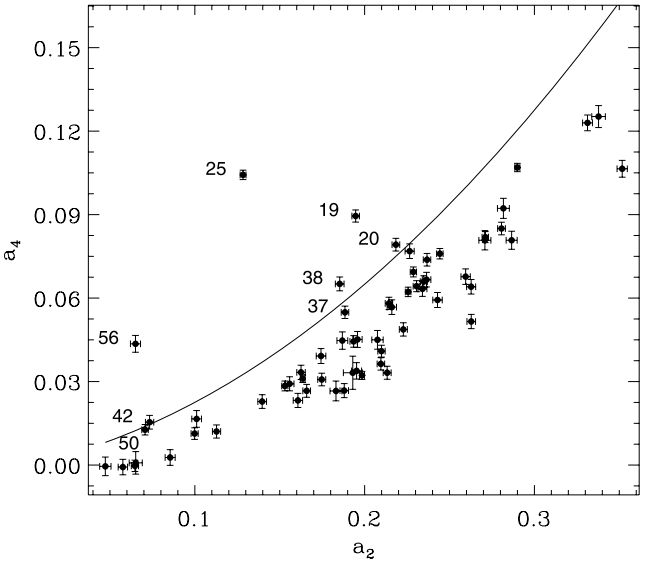


**Figure 5.** Classification of the 62 eclipsing binaries in the $a_2$–$a_4$ plane of Fourier coefficients. Stars lying below the envelope are contact binaries and those lying above it are semidetached and detached binaries. The semidetached and detached binaries in the sample are marked by their serial numbers as in Table 1 corresponding to their respective ASAS IDs and described as in the text.

primary minimum and star 2 at secondary minimum. This notation has been used throughout the text.

The input parameters to the WD code are the mass ratio ($q$), temperature of star 1 $T_1$, the bolometric albedos $A_1 = A_2 = 0.5$ for stars having convective envelopes ($T < 7200$ K) and 1 for radiative envelopes ($T > 7200$ K) and gravity-darkening coefficients $g_1 = g_2 = 0.32$ for convective envelopes and 1.0 for radiative envelopes, following Von Zeipel's law. The monochromatic and bolometric limb-darkening coefficients were interpolated for logarithmic law from van Hamme's table (van Hamme 1993).

The adjustable parameters are the temperature of star 2 $T_2$, orbital inclination ($i$), the surface potentials $\Omega_1$, $\Omega_2$ of the components, and the monochromatic luminosity of star 1 $L_1$. A Planck function was used to compute the luminosity of the star 1. In some cases, third light ($l_3$) was also kept as an adjustable parameter in order to get a better fit of some of the light curves. The third light ($l_3$) is in the unit of total light as implemented in PHOEBE. However, determination of $l_3$ from the photometric light-curve modelling sometimes affects the orbital inclination and amplitude of the light curve. In the two cases 051114−0833.4 and 100141+1724.5, we have found that the determination of third light is highly correlated with the orbital inclination. In these cases, we have chosen $l_3$ as determined from spectroscopy and available in the literature. The values of $l_3$ for these two stars were $0.16 \pm 0.02$ (Pribulla et al. 2009b) and 0.13 (Pribulla et al. 2007), respectively. We have adopted these values of $l_3$ and kept them fixed in the light-curve modelling. In the case of two stars, 073246−2047.5 and 204628−7157.0, we found that their light curves could not be fitted properly, especially the minima, using the $q_{sp}$ values. Therefore, we have also kept spectroscopic mass ratio $q_{sp}$ as an adjustable parameter to get a better fit to these light-curve data. In these two cases, we have used only the adjusted mass

**Table 3.** Fourier parameters of the first eight ASAS eclipsing binaries in the sample of the present study. The full table is available as Supporting Information in the online version of this paper.

| ASAS ID | $m_0$<br>$\sigma m_0$ | $a_1$<br>$\sigma a_1$ | $b_1$<br>$\sigma b_1$ | $a_2$<br>$\sigma a_2$ | $b_2$<br>$\sigma b_2$ | $a_3$<br>$\sigma a_3$ | $b_3$<br>$\sigma b_3$ | $a_4$<br>$\sigma a_4$ | $b_4$<br>$\sigma b_4$ |
|---|---|---|---|---|---|---|---|---|---|
| 003628+2132.3 | 11.100 09 | 0.019 11 | −0.002 21 | 0.183 13 | −0.001 20 | 0.010 04 | −0.000 30 | 0.026 62 | 0.001 28 |
| | 0.002 48 | 0.003 44 | 0.003 59 | 0.003 52 | 0.003 56 | 0.003 44 | 0.003 65 | 0.003 56 | 0.003 48 |
| 011638−3942.5 | 10.460 70 | 0.015 23 | 0.000 84 | 0.225 63 | −0.002 72 | 0.005 52 | 0.001 57 | 0.062 23 | −0.003 77 |
| | 0.001 18 | 0.001 70 | 0.001 64 | 0.001 65 | 0.001 70 | 0.001 63 | 0.001 72 | 0.001 70 | 0.001 65 |
| 012104+0736.3 | 8.654 92 | 0.010 60 | −0.000 76 | 0.155 83 | 0.000 97 | 0.001 68 | −0.000 65 | 0.029 20 | −0.003 53 |
| | 0.001 81 | 0.002 64 | 0.002 49 | 0.002 56 | 0.002 57 | 0.002 61 | 0.002 51 | 0.002 52 | 0.002 58 |
| 014656−0945.1 | 11.001 20 | 0.100 34 | −0.011 79 | 0.228 71 | 0.008 06 | 0.063 91 | 0.000 53 | 0.069 40 | −0.004 23 |
| | 0.001 30 | 0.001 92 | 0.001 76 | 0.001 85 | 0.001 84 | 0.001 86 | 0.001 81 | 0.001 79 | 0.001 88 |
| 014854−2053.6 | 10.534 48 | 0.011 95 | −0.001 06 | 0.289 95 | −0.000 44 | 0.011 28 | −0.000 32 | 0.106 93 | 0.001 90 |
| | 0.001 04 | 0.001 45 | 0.001 49 | 0.001 51 | 0.001 43 | 0.001 46 | 0.001 48 | 0.001 49 | 0.001 46 |
| 023833−1417.9 | 9.635 91 | 0.006 77 | −0.000 58 | 0.259 50 | −0.002 34 | 0.006 05 | 0.000 21 | 0.067 71 | 0.002 20 |
| | 0.001 95 | 0.002 73 | 0.002 80 | 0.002 74 | 0.002 79 | 0.002 81 | 0.002 72 | 0.002 78 | 0.002 75 |
| 024952+0856.3 | 8.800 81 | 0.009 02 | −0.001 16 | 0.101 05 | 0.001 72 | −0.000 95 | 0.000 50 | 0.016 58 | −0.002 35 |
| | 0.002 05 | 0.002 99 | 0.002 83 | 0.002 85 | 0.002 97 | 0.002 97 | 0.002 85 | 0.003 00 | 0.002 83 |
| 030701−5608.1 | 11.141 92 | 0.113 53 | −0.001 13 | 0.236 75 | 0.002 97 | 0.071 94 | 0.002 07 | 0.073 78 | 0.002 89 |
| | 0.001 57 | 0.002 25 | 0.002 20 | 0.002 21 | 0.002 24 | 0.002 21 | 0.002 25 | 0.002 27 | 0.002 18 |

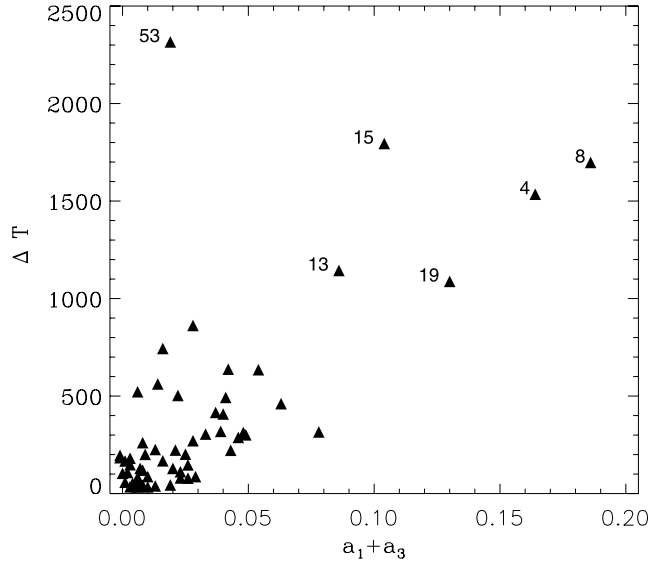


**Figure 6.** Relation between the Fourier coefficients $a_1 + a_3$ and the temperature difference ($\Delta T \geq 1000$ K) obtained from the modelling for the 62 eclipsing binaries in the sample.

ratios. The values of photometric mass ratio $q_{\rm ph}$ obtained for the two cases are $q_{\rm ph} = 0.190 \pm 0.020$ and $0.200 \pm 0.013$, whereas their spectroscopic values were 0.25(3) (Duerbeck & Rucinski 2007) and 0.228(8) (Rucinski & Duerbeck 2006), respectively. In the case of star 073246−2047.5, the $q_{\rm ph}$ value is within $2\sigma$ of $q_{\rm sp}$, whereas for 204628−7157.0, $q_{\rm ph}$ is within $3.5\sigma$ of the $q_{\rm sp}$ value, which may be considered a little higher. These values of $q_{\rm ph}$ were used to model these two stars. We have marked the solutions for these two stars in Table 4. For semidetached binaries, modes 4 and 5 of the WD code were used suitably for the primary and the secondary stars filling their limiting lobes respectively. The fill-out factor ($f$) is given by

$$f = \frac{\Omega_{\rm in} - \Omega_{1,2}}{\Omega_{\rm in} - \Omega_{\rm out}}, \quad (4)$$

where $\Omega_{\rm in}$ and $\Omega_{\rm out}$ refer to the inner and the outer Lagrangian surface potentials, respectively, and $\Omega_{1,2}$ represents the potential of the surface of star 1, 2 respectively. In the case of contact binaries, $\Omega_1 = \Omega_2 = \Omega$, where $\Omega$ is the surface potential of the common envelope for the binary system. For semidetached binaries with the primary component filling its Roche lobe, $\Omega_1 = \Omega_{\rm in}$ and with the secondary filling its Roche lobe $\Omega_2 = \Omega_{\rm in}$. For detached binaries $\Omega_{1,2} > \Omega_{\rm in}$. Therefore, the eclipsing binaries are classified into contact, semidetached and detached binaries according to $0 < f < 1, f = 0$ and $f < 0$, respectively. Contact binaries are classified as A-type if the primary minimum is a transit, and W-type if it is an occultation. Therefore, $M_2/M_1 < 1$ for A-type, $M_2/M_1 > 1$ for W-type contact binaries. The surface temperature difference between the two components is in general less than 1000 K. On the other hand, if the temperature difference between the components $\Delta T \geq 1000$ K, then those contact binaries are sometimes called B-type (Csizmadia & Klagyivik 2004). Lucy & Wilson (1979) first introduced B-type systems which are systems in geometrical contact, but not in thermal contact, and therefore there are large surface temperature differences between the components (Csizmadia & Klagyivik 2004) that produce differences in the levels of the minima. These binaries show an EB ($\beta$ Lyrae)-type light curve, but have an orbital period which falls in the range of classical W UMa systems (Kaluzny 1986). Rucinski (1997a) defined the B-type contact systems as those systems which show large differences in depths of eclipses, yet appear to be in contact and exhibit $\beta$ Lyrae-type light curves. Some of them may be very close, semidetached binaries (ESD) mimicking contact systems and some may be in contact. No attempt has been made to obtain spot parameters for the systems showing the O'Connell (1951) effect. As it has been observed that with the spot solutions included in the WD code, the whole light curve can be easily fitted, but a serious problem of uniqueness of the solution persists (Maceroni & van't Veer 1993) unless other means of investigation such as Doppler imaging techniques are applied (Maceroni et al. 1994). The stars with serial numbers 15, 34, 43, 48 57 and 60 exhibit a typical O'Connell (1951) effect. A reasonable fit to the maxima of the light curves of these stars could be obtained from the light-curve modelling without spots. In this paper, the more massive component is denoted by $M_{\rm P}$, and the less massive component by $M_{\rm S}$. Also, throughout this paper, unless the errors are written otherwise, we express the standard errors in terms of the last quoted digits. For example, 2970.55742(53) should be interpreted as $2970.55742 \pm 0.00053$.

The outputs of the WD differential correction (dc) minimization program as implemented in PHOEBE are the values of the fitting parameters and the formal statistical errors associated with each of the fitting parameters. Sometimes, the error estimates are too optimistic. The values, errors and stability of the solutions were explored using the Monte Carlo parameter scan (heuristic scan) around the best solution using the PHOEBE scripter capability (Bonanos 2009). The WD dc minimization program was run 1000 times, each time updating the input parameter values to the values determined in the previous iteration. The final values for the parameters were determined from the mean of the parameters obtained in 1000 iterations, and the standard deviations were taken as the errors on these parameters. In Fig. 7, we show the histograms of the results obtained using the heuristic scan method for the four parameters fit in the overcontact mode with PHOEBE for the star ASAS 024952+0856.3. For the present sample in this study, we have found that the error estimates of the fitting parameters obtained using the heuristic scan method are reasonable, except for the temperature error $\sigma T_2$, which is unrealistically small and underestimated. In order to obtain a realistic estimate of the error in $T_2$, we derived the values of $T_2$ for two fixed values, $T_1 - \sigma T_1$ and $T_1 + \sigma T_1$, keeping other parameters fixed as obtained for $T_1$ from the modelling, where the value of $\sigma T_1$ is obtained from the colour/spectral type–temperature calibration (Cox 2000) and is listed in Table 4. We then find the temperature differences between the newly obtained values of $T_2$ in the two cases and the $T_2$ value obtained for $T_1$. The mean value of these two temperature differences is taken as the approximate error in $T_2$.

Fig. 8 shows the phased light curves of all 62 stars in the present study. The solid line is the synthetic light curve computed from the WD light-curve modelling technique.

### 5.1 Temperatures

To determine the effective temperatures of the primary components of the programme stars, we used the spectral types of these stars from the literature, mostly from RC. Then, theoretical spectral type–temperature relations (Cox 2000) were used to calculate the temperatures of the primary components. However, when the spectral type is not given in the literature, we used the ($J - K$) colour index from the Two Micron All-Sky Survey (2MASS) catalogue (Cutri et al. 2003) to determine its spectral type using the colour–temperature calibration of Cox (2000). For the majority of stars in the sample, the spectral types were determined by RC either

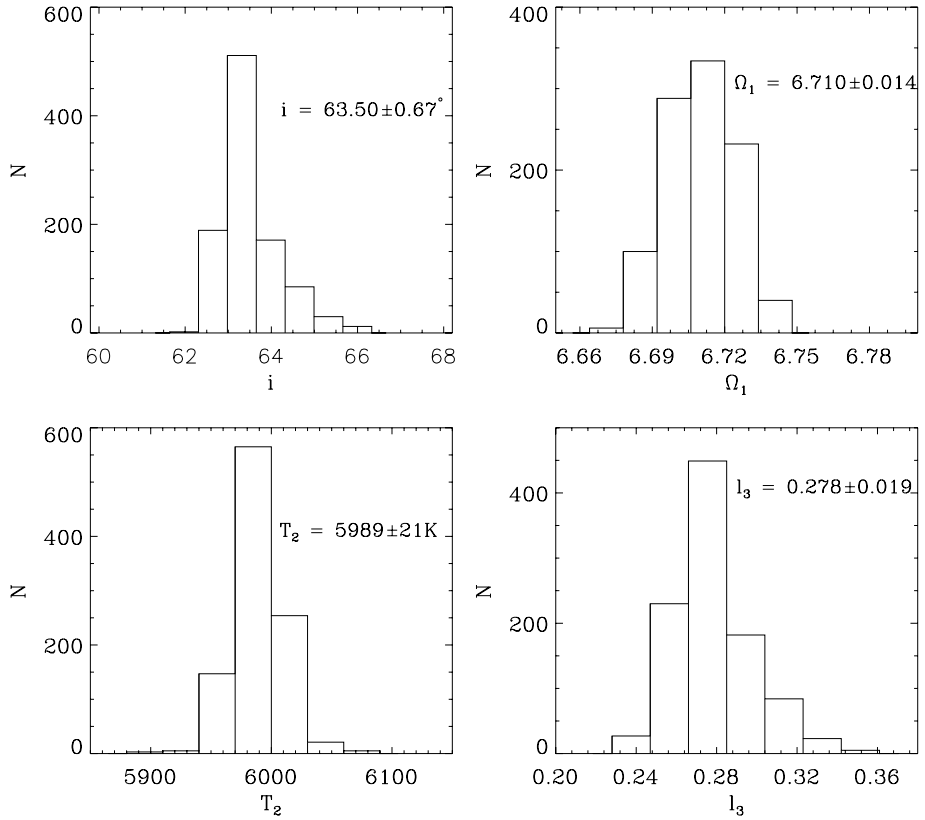


**Figure 7.** Histograms of the results obtained using the Monte Carlo parameter scan for the four parameters fit in the overcontact mode with PHOEBE for the star ASAS 024952+0856.3.

by direct spectral classification or using $(B - V)$ or $(J - K)$ colour index. 2MASS data are very useful for spectral classification on the basis of the observed colours, especially the $(J - K)$ colour, with the advantage that the effect of interstellar reddening is negligible compared to $(B - V)$ and is monotonically rising from the early spectral types to about M0V (Cox 2000; Pribulla et al. 2009b). The temperatures of the secondary components were estimated by using PHOEBE with the temperatures of the primaries fixed. For one star in the sample 110505+0509.1 (Ap Leo), we have not found any spectral classification. In that case, we estimated its spectral type to be F8V corresponding to its infrared colour index $(J - K) = 0.368$ mag. On the other hand, when the spectral classification in RC is given as F5/8V, we take its spectral class as F8V.

### 5.2 Absolute dimensions

In order to calculate the absolute dimensions of the eclipsing binary systems, we used the orbital elements obtained from the spectroscopy as given in the literature. The orbital elements are the velocity semi-amplitudes $(K_1, K_2)$. From the light-curve modelling, we found orbital inclination $i$, temperatures of the secondary components $T_2$, and fractional stellar radii $r_1$, $r_2$. The radii $r_{1,2}$ obtained from the light-curve modelling are normalized to the semimajor axis of the binary system, i.e. $r = R/a$, where $a$ is the semimajor axis and is determined using $i$, $K_1$, $K_2$ and $P$. Period $P$ is that obtained from the ME method. The component radii were taken as the geometrical mean of the polar, side and back radii for contact systems and polar, side, back and point radii for semidetached and detached systems. The luminosities of the two components were calculated from the radii and temperatures by $L_j/L_\odot = (R_j/R_\odot)^2(T_j/5780)^4$, where suffix $j$ refers to either component of the system. The mass function of the system is defined as $f(M) = (M_1 + M_2)\sin^3(i)$, where the total mass of the system $M = (M_1 + M_2)$ in solar units $(M_\odot)$ was obtained using Kepler's third law. Hence the individual masses were obtained using the total mass and the mass ratio. The spectroscopic estimate of the mass function is given by (Rucinski & Lu 1999)

$$f(M) = 1.0385 \times 10^{-7}(K_1 + K_2)^3 P(\mathrm{d})[\mathrm{M}_\odot]. \quad (5)$$

## 6 RESULTS AND COMPARISON WITH THE LITERATURE

In this section, we present determinations of the geometrical and physical parameters of the 62 eclipsing binary stars using the WD code and the orbital elements as given in the literature. Table 4 lists the parameters obtained from the light-curve modelling. In Table 5, we list the physical parameters of all 62 stars determined using the parameters in Table 4 and the radial velocity semi-amplitudes as listed in Table 2.

### 6.1 Comparison with 203113+0513.2 = MR Del

In order to check the quality of the results obtained, we compare the spectral type of the system MR Del (203113+0513.2) as given in Pribulla et al. (2009b) to that determined by us from the light-curve modelling. Pribulla et al. (2009b) predicted a spectral classification (K2V+K6V) for the system. Spectral type K2V is consistent with the infrared colour index of $(J - K) = 0.620$ mag. Assuming this as the spectral type of the primary component, we calculated its temperature as $T_1 = 4830$ K following the calibration of Cox (2000).

**Table 4.** Results obtained from the light-curve modelling.

| ASAS ID | $i(^\circ)$ | $\Omega_1$ | $\Omega_2$ | $x_1$ | $x_2$ | $r_1$ | $r_2$ | $T_1$(K)* | $T_2$(K) | Fill-out | $l_3$ |
|---|---|---|---|---|---|---|---|---|---|---|---|
| 003628+2132.3 | 79.88 ± 1.72 | 1.985 ± 0.010 | 1.985 | 0.72 | 0.72 | 0.587 ± 0.007 | 0.268 ± 0.006 | 6381 ± 182 | 6294 ± 172 | 0.85 | 0 |
| 011638−3942.S | 74.00 ± 0.22 | 6.096 ± 0.008 | 6.096 | 0.73 | 0.73 | 0.307 ± 0.001 | 0.479 ± 0.001 | 5940 ± 149 | 5717 ± 138 | 0.19 | 0 |
| 012104+0736.3 | 69.06 ± 0.80 | 2.253 ± 0.012 | 2.253 | 0.73 | 0.73 | 0.525 ± 0.004 | 0.274 ± 0.005 | 6250 ± 157 | 6024 ± 150 | 0.35 | 0 |
| 014656−0945.1 | 82.25 ± 0.44 | 2.676 ± 0.006 | 2.676 | 0.70 | 0.79 | 0.464 ± 0.001 | 0.310 ± 0.002 | 6765 ± 153 | 5230 ± 93 | 0.08 | 0 |
| 014854−2053.6 | 81.18 ± 0.10 | 3.308 ± 0.002 | 3.308 | 0.73 | 0.73 | 0.357 ± 0.001 | 0.408 ± 0.001 | 5865 ± 152 | 5753 ± 147 | 0.06 | 0 |
| 023833−1417.9 | 82.48 ± 0.34 | 2.529 ± 0.005 | 2.529 | 0.71 | 0.71 | 0.486 ± 0.001 | 0.308 ± 0.002 | 6650 ± 178 | 6611 ± 176 | 0.24 | 0 |
| 024952+0856.3 | 63.50 ± 0.67 | 6.710 ± 0.014 | 6.710 | 0.73 | 0.73 | 0.293 ± 0.001 | 0.494 ± 0.001 | 6250 ± 237 | 5989 ± 220 | 0.02 | 0.278 ± 0.019 |
| 030701−5608.1 | 80.36 ± 0.17 | 2.778 ± 0.006 | 2.778 | 0.70 | 0.79 | 0.455 ± 0.001 | 0.323 ± 0.001 | 6881 ± 169 | 5183 ± 99 | 0.18 | 0 |
| 030953−0653.6 | 75.70 ± 0.23 | 6.065 ± 0.008 | 6.065 | 0.74 | 0.74 | 0.308 ± 0.001 | 0.479 ± 0.001 | 6093 ± 153 | 6006 ± 150 | 0.18 | 0 |
| 033459+1742.6 | 68.10 ± 0.24 | 7.251 ± 0.011 | 7.251 | 0.73 | 0.73 | 0.284 ± 0.001 | 0.503 ± 0.001 | 5940 ± 259 | 5906 ± 254 | 0.18 | 0.013 ± 0.009 |
| 034814+2218.9 | 82.33 ± 0.46 | 2.711 ± 0.006 | 2.711 | 0.73 | 0.73 | 0.464 ± 0.001 | 0.322 ± 0.002 | 5790 ± 128 | 5711 ± 119 | 0.09 | 0 |
| 034928+1254.7 | 74.50 ± 0.69 | 5.057 ± 0.007 | 5.057 | 0.73 | 0.73 | 0.326 ± 0.001 | 0.436 ± 0.001 | 6250 ± 126 | 6082 ± 119 | 0.03 | 0 |
| 035153-1031.8 | 74.50 ± 0.69 | 2.406 ± 0.023 | 2.406 | 0.70 | 0.76 | 0.504 ± 0.007 | 0.298 ± 0.008 | 6881 ± 177 | 5737 ± 122 | 0.37 | 0 |
| 041209−1028.2 | 80.44 ± 0.23 | 5.547 ± 0.008 | 5.547 | 0.73 | 0.73 | 0.318 ± 0.001 | 0.461 ± 0.001 | 5712 ± 145 | 5411 ± 129 | 0.16 | 0 |
| 042925−3334.6 | 69.40 ± 0.25 | 2.337 ± 0.004 | 2.337 | 0.70 | 0.80 | 0.525 ± 0.002 | 0.326 ± 0.002 | 6881 ± 196 | 5086 ± 104 | 0.71 | 0 |
| 051114−0833.4 | 82.08 ± 0.44 | 4.430 ± 0.029 | 4.430 | 0.72 | 0.74 | 0.360 ± 0.004 | 0.433 ± 0.004 | 6250 ± 153 | 5931 ± 134 | 0.25 | 0.16 ± 0.02 [a] |
| 051832−6813.6 | 76.32 ± 0.15 | 4.556 ± 0.013 | 4.556 | 0.73 | 0.73 | 0.351 ± 0.002 | 0.432 ± 0.002 | 5560 ± 116 | 5272 ± 103 | 0.20 | 0 |
| 062605+2759.9 | 76.28 ± 0.90 | 2.081 ± 0.007 | 2.081 | 0.72 | 0.72 | 0.563 ± 0.003 | 0.271 ± 0.004 | 6381 ± 134 | 6416 ± 135 | 0.66 | 0 |
| 064558−0017.5 | 89.00 ± 2.60 | 3.190 | 3.343 ± 0.052 | 0.72 | 0.80 | 0.442 ± 0.002 | 0.327 ± 0.010 | 6250 ± 157 | 5162 ± 109 | 0.00 | 0.242 ± 0.027 |
| 071058−0352.8 | 74.85 ± 0.07 | 4.037 ± 0.011 | 3.701 | 0.71 | 0.72 | 0.342 ± 0.002 | 0.402 ± 0.002 | 7640 ± 174 | 7744 ± 182 | 0.00 | 0 |
| 073246−2047.5 | 84.47 ± 0.58 | 2.121 ± 0.002 | 2.121 | 0.70 | 0.70 | 0.557 ± 0.001 | 0.284 ± 0.001 | 6881 ± 315 | 6801 ± 304 | 0.71 | 0 † |
| 073338−5007.4 | 79.47 ± 0.73 | 2.134 ± 0.004 | 2.134 | 0.71 | 0.71 | 0.553 ± 0.002 | 0.278 ± 0.002 | 6514 ± 144 | 6662 ± 148 | 0.57 | 0 |
| 073905−0239.1 | 72.14 ± 0.27 | 2.512 ± 0.005 | 2.512 | 0.70 | 0.70 | 0.496 ± 0.002 | 0.329 ± 0.002 | 7000 ± 191 | 6584 ± 169 | 0.49 | 0 |
| 084002+1900.0 | 62.19 ± 0.48 | 5.427 ± 0.021 | 5.427 | 0.73 | 0.73 | 0.323 ± 0.003 | 0.460 ± 0.002 | 6250 ± 127 | 6121 ± 120 | 0.23 | 0 |
| 084108−3212.1 | 90.10 ± 0.97 | 6.004 ± 0.056 | 6.640 ± 0.095 | 0.67 | 0.67 | 0.200 ± 0.002 | 0.172 ± 0.002 | 7468 ± 203 | 7521 ± 208 | <0 | 0 |
| 100141+1724.5 | 68.63 ± 0.37 | 4.214 ± 0.022 | 4.214 | 0.75 | 0.75 | 0.368 ± 0.003 | 0.423 ± 0.003 | 5150 ± 118 | 4742 ± 248 | 0.25 | 0.13 [b] |
| 100234+1702.8 | 77.16 ± 0.42 | 2.471 ± 0.010 | 2.471 | 0.69 | 0.69 | 0.500 ± 0.003 | 0.321 ± 0.004 | 7300 ± 170 | 7265 ± 167 | 0.40 | 0 |
| 100248+0105.7 | 79.12 ± 0.44 | 2.146 ± 0.009 | 2.146 | 0.70 | 0.72 | 0.550 ± 0.003 | 0.279 ± 0.005 | 6650 ± 163 | 6448 ± 153 | 0.52 | 0.114 ± 0.011 |
| 101602−0618.5 | 74.88 ± 0.65 | 1.928 ± 0.002 | 1.928 | 0.70 | 0.72 | 0.594 ± 0.001 | 0.221 ± 0.001 | 6881 ± 199 | 6378 ± 169 | 0.42 | 0 |
| 104033+1334.0 | 84.05 ± 0.89 | 2.374 ± 0.004 | 2.374 | 0.69 | 0.69 | 0.514 ± 0.002 | 0.313 ± 0.002 | 7148 ± 163 | 7158 ± 167 | 0.83 | 0 |
| 105030−0241.7 | 65.53 ± 0.18 | 6.720 ± 0.007 | 6.720 | 0.73 | 0.73 | 0.294 ± 0.001 | 0.493 ± 0.001 | 5960 ± 182 | 5877 ± 176 | 0.20 | 0 |
| 110211+0953.7 | 73.85 ± 0.15 | 5.400 ± 0.006 | 5.400 | 0.70 | 0.70 | 0.324 ± 0.001 | 0.460 ± 0.001 | 6650 ± 148 | 6616 ± 144 | 0.18 | 0 |
| 110505+0509.1 | 79.66 ± 0.65 | 2.404 ± 0.012 | 2.404 | 0.73 | 0.73 | 0.503 ± 0.004 | 0.295 ± 0.004 | 6250 ± 155 | 6247 ± 156 | 0.37 | 0 |
| 120103+1300.5 | 72.54 ± 0.30 | 2.547 ± 0.006 | 2.547 | 0.70 | 0.70 | 0.489 ± 0.002 | 0.324 ± 0.002 | 8180 ± 188 | 7542 ± 167 | 0.40 | 0 |
| 121206+2232.0 | 90.58 ± 2.85 | 4.982 ± 0.027 | 4.982 | 0.79 | 0.79 | 0.338 ± 0.004 | 0.450 ± 0.003 | 4546 ± 72 | 4399 ± 67 | 0.04 | 0 |
| 123300+2642.9 | 72.43 ± 0.29 | 5.319 ± 0.009 | 5.319 | 0.77 | 0.77 | 0.326 ± 0.001 | 0.457 ± 0.001 | 4830 ± 115 | 4517 ± 98 | 0.15 | 0 |
| 131032−0409.5 | 68.91 ± 0.22 | 4.231 ± 0.019 | 4.207 | 0.77 | 0.77 | 0.382 ± 0.003 | 0.428 ± 0.001 | 4830 ± 136 | 4559 ± 121 | 0.00 | 0 |
| 134607+0506.9 | 79.06 ± 0.43 | 3.437 | 4.998 ± 0.077 | 0.73 | 0.73 | 0.356 ± 0.002 | 0.360 ± 0.001 | 6250 ± 145 | 6211 ± 146 | 0.00 | 0 |
| 141726+1234.1 | 77.29 ± 0.39 | 2.698 ± 0.014 | 2.698 | 0.73 | 0.73 | 0.463 ± 0.003 | 0.316 ± 0.004 | 5560 ± 120 | 5099 ± 101 | 0.12 | 0 |
| 141937+0553.8 | 65.52 ± 0.43 | 2.696 ± 0.017 | 2.696 | 0.69 | 0.69 | 0.482 ± 0.005 | 0.362 ± 0.006 | 7148 ± 198 | 7201 ± 203 | 0.60 | 0 |
| 143504+0906.8 | 60.87 ± 0.89 | 1.924 ± 0.004 | 1.924 | 0.73 | 0.73 | 0.601 ± 0.001 | 0.255 ± 0.004 | 6250 ± 219 | 6234 ± 216 | 0.91 | 0 |
| 144803+1356.7 | 73.96 ± 1.00 | 2.348 | 2.978 ± 0.086 | 0.70 | 0.70 | 0.535 ± 0.002 | 0.157 ± 0.009 | 6650 ± 175 | 6846 ± 187 | 0.00 | 0.302 ± 0.036 |
| 152243+1615.7 | 50.47 ± 2.24 | 2.090 ± 0.017 | 2.090 | 0.73 | 0.73 | 0.552 ± 0.005 | 0.260 ± 0.006 | 5940 ± 144 | 5759 ± 283 | 0.68 | 0 |
| 153152−1541.1 | 90.35 ± 2.40 | 2.479 ± 0.007 | 2.479 | 0.73 | 0.73 | 0.492 ± 0.002 | 0.302 ± 0.002 | 5790 ± 162 | 5974 ± 166 | 0.29 | 0.207 ± 0.008 |
| 155649+2216.0 | 83.85 ± 0.67 | 3.157 ± 0.058 | 3.157 | 0.73 | 0.73 | 0.446 ± 0.007 | 0.349 ± 0.007 | 5636 ± 108 | 5320 ± 92 | 0.46 | 0 |
| 164121+0030.4 | 69.77 ± 0.21 | 6.397 ± 0.013 | 6.397 | 0.73 | 0.73 | 0.307 ± 0.002 | 0.495 ± 0.001 | 5940 ± 136 | 5739 ± 129 | 0.22 | 0 |
| 165717+1059.8 | 47.05 ± 0.68 | 2.261 ± 0.007 | 2.261 | 0.73 | 0.73 | 0.525 ± 0.002 | 0.267 ± 0.001 | 5560 ± 135 | 5440 ± 127 | 0.21 | 0 |
| 171358+1621.0 | 88.69 ± 5.29 | 2.374 ± 0.029 | 2.374 | 0.70 | 0.74 | 0.506 ± 0.009 | 0.286 ± 0.001 | 6765 ± 168 | 6130 ± 139 | 0.30 | 0 |
| 173356+0810.0 | 44.06 ± 1.24 | 5.954 ± 0.027 | 5.954 | 0.73 | 0.73 | 0.303 ± 0.003 | 0.465 ± 0.003 | 5940 ± 165 | 5418 ± 332 | 0.14 | 0 |
| 175332−0354.9 | 57.97 ± 0.31 | 2.505 ± 0.007 | 2.446 | 0.73 | 0.73 | 0.491 ± 0.003 | 0.299 ± 0.001 | 5940 ± 151 | 5773 ± 144 | 0.00 | 0.144 ± 0.008 |
| 180921+0909.1 | 80.19 ± 0.25 | 2.363 ± 0.003 | 2.363 | 0.71 | 0.71 | 0.518 ± 0.001 | 0.320 ± 0.001 | 6381 ± 135 | 6424 ± 136 | 0.61 | 0 |
| 182913+0647.3 | 66.36 ± 0.48 | 6.991 ± 0.023 | 6.991 | 0.72 | 0.72 | 0.301 ± 0.003 | 0.514 ± 0.002 | 6381 ± 191 | 6273 ± 180 | 0.56 | 0 |
| 185318+2113.5 | 41.59 ± 2.78 | 2.569 ± 0.034 | 2.569 | 0.72 | 0.80 | 0.481 ± 0.009 | 0.311 ± 0.010 | 7816 ± 173 | 5500 ± 623 | 0.41 | 0 |
| 193524+0550.3 | 82.47 ± 0.22 | 6.160 ± 0.005 | 6.160 | 0.72 | 0.72 | 0.307 ± 0.001 | 0.483 ± 0.001 | 6381 ± 153 | 6252 ± 147 | 0.24 | 0 |
| 194813+0918.5 | 93.81 ± 0.22 | 3.384 ± 0.006 | 3.384 | 0.74 | 0.75 | 0.413 ± 0.001 | 0.384 ± 0.001 | 6093 ± 152 | 5871 ± 140 | 0.24 | 0 |
| 203113+0513.2 | 77.06 ± 1.76 | 6.017 ± 0.591 | 4.384 ± 0.094 | 0.77 | 0.77 | 0.200 ± 0.021 | 0.281 ± 0.008 | 4830 ± 94 | 4337 ± 68 | <0 | 0 |
| 204628−7157.0 | 84.81 ± 0.60 | 2.147 ± 0.003 | 2.147 | 0.70 | 0.70 | 0.552 ± 0.001 | 0.287 ± 0.002 | 6881 ± 160 | 6837 ± 158 | 0.52 | 0.089 ± 0.005 † |
| 205710+1939.0 | 45.25 ± 2.45 | 6.051 ± 0.080 | 6.051 | 0.73 | 0.75 | 0.308 ± 0.009 | 0.478 ± 0.008 | 6250 ± 185 | 6192 ± 168 | 0.09 | 0 |
| 222257+1619.4 | 87.96 ± 2.59 | 6.142 ± 0.012 | 6.142 | 0.72 | 0.74 | 0.311 ± 0.001 | 0.487 ± 0.002 | 6381 ± 126 | 6076 ± 113 | 0.32 | 0 |
| 233655+1548.1 | 71.11 ± 0.67 | 2.240 ± 0.009 | 2.240 | 0.70 | 0.71 | 0.470 ± 0.003 | 0.312 ± 0.003 | 7300 ± 184 | 6438 ± 141 | 0.81 | 0 |
| 234535+2528.3 | 73.23 ± 0.33 | 2.640 ± 0.012 | 2.640 | 0.69 | 0.69 | 0.541 ± 0.003 | 0.319 ± 0.006 | 7000 ± 192 | 6438 ± 161 | 0.10 | 0 |
| 234718−0805.2 | 70.36 ± 0.32 | 2.177 ± 0.004 | 2.177 | 0.70 | 0.70 | 0.542 ± 0.002 | 0.276 ± 0.002 | 6881 ± 182 | 6137 ± 140 | 0.48 | 0 |

*The errors in $T_1$ are obtained from the colour/spectral type-temperature calibration (Cox 2000) and are not obtained from the modelling. †The solutions are obtained using the $q_{\rm ph}$ values as described in the text. [a]Pribulla et al. (2009b), [b]Pribulla et al. (2007).

From the light-curve modelling, we found the temperature of the secondary component as $T_2 = 4337 \pm 68$ K, which is consistent with the spectral type K6V for the secondary component as estimated by Pribulla et al. (2009b).

We also compare the determination of physical parameters of 23 stars common to our sample with previous recent publications. We list all 23 stars in Table 6 and their physical parameters along with the references in the literature. In Fig. 9, we show scatter plots

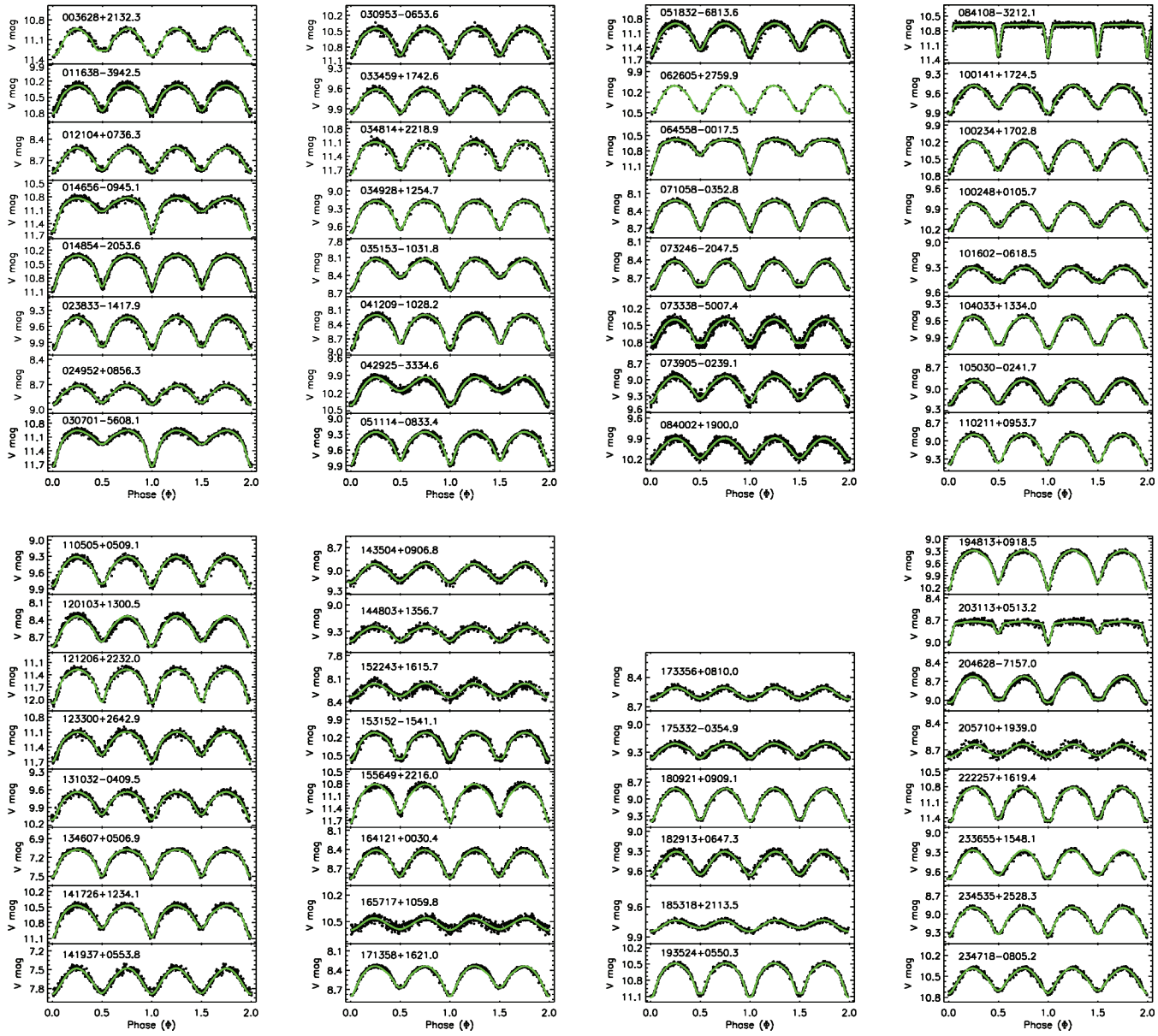


**Figure 8.** Phased light curves of all 62 stars in the present study. The solid line is the synthetic light curve computed from the WD light-curve modelling technique. The parameters obtained from the modelling are listed in Table 4.

between the parameters determined by us (shown on the *x*-axis and represented by 'DS' in parentheses) and those in the literature (shown on the *y*-axis and represented by 'Lit' in parentheses). From Fig. 9, it seems that the errors in $L_1$ and $L_2$ were underestimated in some of the cases in the literature and their calculations were not clearly mentioned. The clustering of data points along a straight line of zero intercept and unit slope indicates a positive linear correlation with the presence of three outliers. The ASAS IDs of these stars are 024952+0856.3 (EE Cet), 071058−0352.8 (V753 Mon) and 171358+1621.0 (AK Her). We discuss these stars in the following subsections in view of mismatch in their parameter determinations.

### 6.2 ASAS 024952+0856.3 = EE Cet

Variability of the combined light of the visual binary ADS 2163 was discovered by the *Hipparcos* satellite mission (Perryman & ESA 1997). The system shows a light-curve variation with an amplitude of 0.23 mag and a 0.38-d period in the *Hipparcos* photometric observations. Rucinski et al. (2002) correctly found that the source of variability is the southern, fainter companion, which is classified as a W UMa type eclipsing binary EE Cet ($P \sim 0.38$ d). In their radial velocity study, EE Cet was observed without contamination by the northern companion, separated by 5.6 arcsec. They assigned a spectral class F8V to the system and classified it as a W-type W UMa binary with a mass ratio $q_{\rm sp} = 0.315(5)$. A photometric study of this star was carried out by Djurašević et al. (2006) using $q = 0.315$, who obtained the parameters as listed in Table 7. They obtained $i(^\circ) = 78.5 \pm 0.2$, $M_1 + M_2 = 1.80\,{\rm M}_\odot$, $L_3 \sim 0.54$ and mass function $f(M) = 1.694\,{\rm M}_\odot$. This value of $f(M) = 1.694\,{\rm M}_\odot$ is quite close to the spectroscopically determined value $1.706(41)\,{\rm M}_\odot$ of Rucinski et al. (2002). We have also used the same value of $q_{\rm sp} = 0.315$ to model the ASAS light curve. Since the star is a W-type contact binary, we have used the inverse of $q_{\rm sp}$ in the photometric

**Table 5.** Physical parameters of the 62 eclipsing binary stars.

| ID | $a$ /R$_\odot$ | $M$/M$_\odot$ | $f(M)$/M$_\odot$ | $M_1$/M$_\odot$ | $M_2$/M$_\odot$ | $R_1$/R$_\odot$ | $R_2$/R$_\odot$ | $L_1$/L$_\odot$ | $L_2$/L$_\odot$ |
|---|---|---|---|---|---|---|---|---|---|
| 003628+2132.3 | 2.490 ± 0.039 | 1.542 ± 0.070 | 1.471 ± 0.071 | 1.358 ± 0.055 | 0.185 ± 0.020 | 1.462 ± 0.029 | 0.667 ± 0.018 | 3.174 ± 0.487 | 0.626 ± 0.103 |
| 011638−3942.5 | 2.592 ± 0.027 | 1.616 ± 0.049 | 1.435 ± 0.044 | 0.436 ± 0.041 | 1.179 ± 0.151 | 0.796 ± 0.009 | 1.242 ± 0.013 | 0.706 ± 0.086 | 1.476 ± 0.174 |
| 012104+0736.3 | 3.253 ± 0.026 | 2.037 ± 0.048 | 1.659 ± 0.047 | 1.661 ± 0.026 | 0.375 ± 0.010 | 1.708 ± 0.019 | 0.891 ± 0.018 | 3.987 ± 0.489 | 0.937 ± 0.131 |
| 014656−0945.1 | 3.726 ± 0.280 | 2.932 ± 0.644 | 2.852 ± 0.627 | 2.109 ± 0.264 | 0.823 ± 0.215 | 1.729 ± 0.130 | 1.155 ± 0.087 | 5.608 ± 1.352 | 0.894 ± 0.199 |
| 014854−2053.6 | 2.329 ± 0.032 | 1.685 ± 0.067 | 1.625 ± 0.065 | 0.722 ± 0.053 | 0.963 ± 0.097 | 0.831 ± 0.012 | 0.950 ± 0.013 | 0.733 ± 0.097 | 0.886 ± 0.115 |
| 023833−1417.9 | 3.046 ± 0.027 | 1.948 ± 0.051 | 1.898 ± 0.050 | 1.436 ± 0.034 | 0.511 ± 0.025 | 1.480 ± 0.014 | 0.938 ± 0.010 | 3.840 ± 0.482 | 1.507 ± 0.194 |
| 024952+0856.3 | 2.948 ± 0.024 | 2.377 ± 0.056 | 1.704 ± 0.050 | 0.569 ± 0.029 | 1.808 ± 0.126 | 0.864 ± 0.008 | 1.456 ± 0.012 | 1.020 ± 0.173 | 2.445 ± 0.400 |
| 030701−5608.1 | 4.277 ± 0.189 | 2.680 ± 0.345 | 2.568 ± 0.330 | 1.823 ± 0.159 | 0.857 ± 0.147 | 1.946 ± 0.086 | 1.381 ± 0.061 | 7.605 ± 1.419 | 1.234 ± 0.203 |
| 030953−0653.6 | 3.069 ± 0.022 | 1.952 ± 0.041 | 1.776 ± 0.038 | 0.530 ± 0.027 | 1.421 ± 0.098 | 0.945 ± 0.008 | 1.470 ± 0.011 | 1.103 ± 0.128 | 2.519 ± 0.290 |
| 033459+1742.6 | 2.779 ± 0.011 | 1.796 ± 0.021 | 1.435 ± 0.018 | 0.392 ± 0.015 | 1.404 ± 0.070 | 0.789 ± 0.004 | 1.398 ± 0.006 | 0.695 ± 0.129 | 2.130 ± 0.385 |
| 034814+2218.9 | 2.500 ± 0.019 | 1.795 ± 0.041 | 1.747 ± 0.040 | 1.245 ± 0.028 | 0.550 ± 0.021 | 1.160 ± 0.009 | 0.805 ± 0.008 | 1.355 ± 0.142 | 0.618 ± 0.064 |
| 034928+1254.7 | 2.349 ± 0.014 | 1.862 ± 0.032 | 1.666 ± 0.033 | 0.648 ± 0.021 | 1.214 ± 0.054 | 0.766 ± 0.005 | 1.024 ± 0.006 | 0.802 ± 0.075 | 1.286 ± 0.117 |
| 035153−1031.8 | 2.990 ± 0.108 | 1.388 ± 0.146 | 1.242 ± 0.132 | 1.068 ± 0.123 | 0.320 ± 0.057 | 1.507 ± 0.058 | 0.891 ± 0.040 | 4.561 ± 0.822 | 0.770 ± 0.135 |
| 041209−1028.2 | 2.257 ± 0.022 | 1.489 ± 0.043 | 1.428 ± 0.041 | 0.426 ± 0.036 | 1.063 ± 0.115 | 0.718 ± 0.007 | 1.041 ± 0.010 | 0.491 ± 0.060 | 0.832 ± 0.096 |
| 042925−3334.6 | 3.987 ± 0.674 | 2.110 ± 1.041 | 1.730 ± 0.854 | 1.623 ± 0.577 | 0.487 ± 0.320 | 2.093 ± 0.354 | 1.300 ± 0.220 | 8.801 ± 3.978 | 1.013 ± 0.425 |
| 051114−0833.4 | 3.159 ± 0.028 | 2.354 ± 0.061 | 2.288 ± 0.060 | 0.933 ± 0.034 | 1.422 ± 0.078 | 1.137 ± 0.016 | 1.368 ± 0.018 | 1.768 ± 0.223 | 2.074 ± 0.241 |
| 051832−6813.6 | 2.020 ± 0.034 | 1.354 ± 0.066 | 1.242 ± 0.061 | 0.523 ± 0.063 | 0.830 ± 0.128 | 0.709 ± 0.013 | 0.873 ± 0.015 | 0.430 ± 0.051 | 0.527 ± 0.059 |
| 062605+2759.9 | 3.289 ± 0.033 | 1.951 ± 0.057 | 1.789 ± 0.056 | 1.669 ± 0.034 | 0.282 ± 0.013 | 1.852 ± 0.021 | 0.891 ± 0.016 | 5.094 ± 0.544 | 1.206 ± 0.145 |
| 064558−0017.5 | 3.734 ± 0.050 | 2.160 ± 0.084 | 2.159 ± 0.084 | 1.294 ± 0.051 | 0.867 ± 0.059 | 1.650 ± 0.023 | 1.221 ± 0.041 | 3.724 ± 0.479 | 0.949 ± 0.143 |
| 071058−0352.8 | 4.814 ± 0.019 | 3.258 ± 0.038 | 2.930 ± 0.034 | 1.654 ± 0.016 | 1.604 ± 0.028 | 1.646 ± 0.012 | 1.935 ± 0.012 | 8.274 ± 0.871 | 12.067 ± 1.288 |
| 073246−2047.5 | 4.396 ± 0.266 | 1.694 ± 0.300 | 1.671 ± 0.296 | 1.422 ± 0.205 | 0.272 ± 0.079 | 2.448 ± 0.148 | 1.248 ± 0.076 | 12.041 ± 3.665 | 2.987 ± 0.897 |
| 073338−5007.4 | 2.746 ± 0.201 | 1.482 ± 0.317 | 1.408 ± 0.301 | 1.245 ± 0.270 | 0.237 ± 0.125 | 1.519 ± 0.111 | 0.763 ± 0.056 | 3.721 ± 0.875 | 1.029 ± 0.243 |
| 073905−0239.1 | 4.453 ± 0.039 | 2.907 ± 0.074 | 2.507 ± 0.065 | 2.117 ± 0.032 | 0.790 ± 0.029 | 2.209 ± 0.021 | 1.465 ± 0.016 | 10.494 ± 1.347 | 3.614 ± 0.448 |
| 084002+1900.0 | 2.762 ± 0.016 | 1.924 ± 0.033 | 1.331 ± 0.029 | 0.602 ± 0.020 | 1.322 ± 0.057 | 0.892 ± 0.010 | 1.271 ± 0.009 | 1.088 ± 0.112 | 2.030 ± 0.189 |
| 084108−3212.1 | 11.791 ± 0.119 | 4.083 ± 0.120 | 4.083 ± 0.120 | 2.078 ± 0.040 | 2.005 ± 0.079 | 2.358 ± 0.033 | 2.028 ± 0.031 | 15.499 ± 2.125 | 11.792 ± 1.667 |
| 100141+1724.5 | 2.071 ± 0.011 | 1.473 ± 0.022 | 1.190 ± 0.020 | 0.621 ± 0.020 | 0.852 ± 0.035 | 0.762 ± 0.007 | 0.876 ± 0.008 | 0.366 ± 0.041 | 0.348 ± 0.079 |
| 100234+1702.8 | 3.505 ± 0.032 | 2.422 ± 0.064 | 2.245 ± 0.061 | 1.797 ± 0.033 | 0.625 ± 0.025 | 1.752 ± 0.019 | 1.125 ± 0.017 | 7.813 ± 0.898 | 3.159 ± 0.388 |
| 100248+0105.7 | 2.850 ± 0.031 | 1.758 ± 0.056 | 1.665 ± 0.054 | 1.471 ± 0.040 | 0.287 ± 0.020 | 1.568 ± 0.019 | 0.795 ± 0.017 | 4.305 ± 0.528 | 0.979 ± 0.134 |
| 101602−0618.5 | 3.148 ± 0.021 | 1.431 ± 0.028 | 1.288 ± 0.028 | 1.301 ± 0.022 | 0.130 ± 0.006 | 1.870 ± 0.013 | 0.696 ± 0.006 | 7.021 ± 0.909 | 0.717 ± 0.088 |
| 104033+1334.0 | 4.212 ± 0.028 | 2.619 ± 0.051 | 2.577 ± 0.051 | 2.010 ± 0.024 | 0.609 ± 0.017 | 2.165 ± 0.017 | 1.318 ± 0.012 | 10.964 ± 1.168 | 4.089 ± 0.457 |
| 105030−0241.7 | 3.004 ± 0.016 | 1.846 ± 0.029 | 1.392 ± 0.022 | 0.440 ± 0.019 | 1.406 ± 0.080 | 0.883 ± 0.006 | 1.481 ± 0.008 | 0.882 ± 0.119 | 2.345 ± 0.308 |
| 110211+0953.7 | 2.770 ± 0.012 | 2.126 ± 0.026 | 1.884 ± 0.024 | 0.669 ± 0.016 | 1.457 ± 0.048 | 0.897 ± 0.005 | 1.274 ± 0.006 | 1.411 ± 0.140 | 2.787 ± 0.269 |
| 110505+0509.1 | 2.954 ± 0.033 | 1.864 ± 0.060 | 1.775 ± 0.058 | 1.437 ± 0.040 | 0.427 ± 0.025 | 1.486 ± 0.020 | 0.872 ± 0.015 | 3.019 ± 0.382 | 1.037 ± 0.140 |
| 120103+1300.5 | 4.501 ± 0.031 | 2.956 ± 0.059 | 2.566 ± 0.053 | 2.139 ± 0.024 | 0.817 ± 0.021 | 2.201 ± 0.018 | 1.458 ± 0.013 | 19.432 ± 2.096 | 6.165 ± 0.660 |
| 121206+2232.0 | 1.580 ± 0.008 | 1.085 ± 0.015 | 1.084 ± 0.015 | 0.374 ± 0.018 | 0.710 ± 0.043 | 0.534 ± 0.007 | 0.711 ± 0.006 | 0.109 ± 0.010 | 0.170 ± 0.013 |
| 123300+2642.9 | 1.723 ± 0.009 | 1.216 ± 0.019 | 1.053 ± 0.017 | 0.389 ± 0.020 | 0.826 ± 0.054 | 0.562 ± 0.004 | 0.787 ± 0.005 | 0.154 ± 0.017 | 0.231 ± 0.023 |
| 131032−0409.5 | 2.313 ± 0.008 | 1.710 ± 0.017 | 1.389 ± 0.015 | 0.745 ± 0.013 | 0.964 ± 0.023 | 0.883 ± 0.008 | 0.990 ± 0.004 | 0.381 ± 0.049 | 0.379 ± 0.043 |
| 134607+0506.9 | 3.105 ± 0.012 | 2.412 ± 0.028 | 2.283 ± 0.029 | 1.331 ± 0.015 | 1.081 ± 0.021 | 1.105 ± 0.008 | 1.118 ± 0.005 | 1.671 ± 0.178 | 1.666 ± 0.173 |
| 141726+1234.1 | 2.348 ± 0.011 | 1.479 ± 0.020 | 1.373 ± 0.020 | 1.036 ± 0.017 | 0.443 ± 0.012 | 1.087 ± 0.009 | 0.742 ± 0.010 | 1.012 ± 0.103 | 0.333 ± 0.035 |
| 141937+0553.8 | 3.574 ± 0.019 | 2.645 ± 0.042 | 1.994 ± 0.037 | 1.774 ± 0.019 | 0.871 ± 0.017 | 1.723 ± 0.020 | 1.294 ± 0.023 | 6.941 ± 0.931 | 4.033 ± 0.595 |
| 143504+0906.8 | 2.550 ± 0.026 | 1.760 ± 0.053 | 1.173 ± 0.047 | 1.584 ± 0.034 | 0.176 ± 0.008 | 1.533 ± 0.016 | 0.650 ± 0.012 | 3.211 ± 0.518 | 0.572 ± 0.101 |
| 144803+1356.7 | 2.754 ± 0.026 | 1.633 ± 0.044 | 1.450 ± 0.045 | 1.309 ± 0.033 | 0.325 ± 0.017 | 1.473 ± 0.015 | 0.432 ± 0.025 | 3.804 ± 0.477 | 0.368 ± 0.083 |
| 152243+1615.7 | 2.093 ± 0.068 | 1.393 ± 0.132 | 0.639 ± 0.087 | 1.187 ± 0.099 | 0.205 ± 0.020 | 1.155 ± 0.039 | 0.544 ± 0.022 | 1.488 ± 0.245 | 0.292 ± 0.081 |
| 153152−1541.1 | 2.384 ± 0.042 | 1.414 ± 0.073 | 1.413 ± 0.073 | 1.063 ± 0.065 | 0.351 ± 0.039 | 1.173 ± 0.021 | 0.720 ± 0.014 | 1.385 ± 0.205 | 0.592 ± 0.088 |
| 155649+2216.0 | 2.572 ± 0.015 | 1.526 ± 0.026 | 1.499 ± 0.026 | 0.893 ± 0.022 | 0.633 ± 0.023 | 1.147 ± 0.019 | 0.898 ± 0.019 | 1.190 ± 0.131 | 0.578 ± 0.064 |
| 164121+0030.4 | 3.150 ± 0.014 | 2.035 ± 0.027 | 1.681 ± 0.023 | 0.511 ± 0.017 | 1.524 ± 0.071 | 0.967 ± 0.008 | 1.559 ± 0.008 | 1.043 ± 0.112 | 2.362 ± 0.236 |
| 165717+1059.8 | 2.641 ± 0.047 | 1.428 ± 0.075 | 0.560 ± 0.035 | 1.160 ± 0.061 | 0.268 ± 0.025 | 1.386 ± 0.025 | 0.705 ± 0.013 | 1.646 ± 0.220 | 0.390 ± 0.051 |
| 171358+1621.0 | 2.711 ± 0.022 | 1.501 ± 0.035 | 1.500 ± 0.037 | 1.175 ± 0.028 | 0.326 ± 0.014 | 1.372 ± 0.027 | 0.775 ± 0.007 | 3.531 ± 0.489 | 0.760 ± 0.082 |
| 173356+0810.0 | 2.695 ± 0.061 | 1.448 ± 0.096 | 0.487 ± 0.046 | 0.410 ± 0.071 | 1.038 ± 0.192 | 0.817 ± 0.020 | 1.253 ± 0.030 | 0.744 ± 0.120 | 1.212 ± 0.355 |
| 175332−0354.9 | 3.181 ± 0.031 | 2.368 ± 0.067 | 1.443 ± 0.044 | 1.834 ± 0.036 | 0.534 ± 0.026 | 1.562 ± 0.018 | 0.951 ± 0.010 | 2.720 ± 0.339 | 0.900 ± 0.108 |
| 180921+0909.1 | 2.984 ± 0.020 | 2.127 ± 0.041 | 2.035 ± 0.040 | 1.630 ± 0.024 | 0.497 ± 0.016 | 1.546 ± 0.011 | 0.955 ± 0.007 | 3.550 ± 0.350 | 1.392 ± 0.138 |
| 182913+0647.3 | 2.598 ± 0.013 | 1.666 ± 0.025 | 1.281 ± 0.024 | 0.370 ± 0.017 | 1.295 ± 0.073 | 0.782 ± 0.009 | 1.335 ± 0.009 | 0.908 ± 0.129 | 2.473 ± 0.315 |
| 185318+2113.5 | 3.470 ± 0.191 | 2.299 ± 0.369 | 0.672 ± 0.154 | 1.675 ± 0.169 | 0.625 ± 0.073 | 1.669 ± 0.097 | 1.079 ± 0.069 | 9.317 ± 1.907 | 0.955 ± 0.554 |
| 193524+0550.3 | 2.699 ± 0.023 | 1.920 ± 0.048 | 1.871 ± 0.047 | 0.510 ± 0.031 | 1.410 ± 0.113 | 0.829 ± 0.008 | 1.304 ± 0.012 | 1.020 ± 0.117 | 2.327 ± 0.260 |
| 194813+0918.5 | 3.355 ± 0.015 | 1.969 ± 0.025 | 1.956 ± 0.025 | 1.067 ± 0.017 | 0.902 ± 0.023 | 1.386 ± 0.007 | 1.288 ± 0.007 | 2.371 ± 0.260 | 1.767 ± 0.187 |
| 203113+0513.2 | 3.009 ± 0.029 | 1.340 ± 0.037 | 1.240 ± 0.043 | 0.700 ± 0.034 | 0.640 ± 0.040 | 0.602 ± 0.063 | 0.845 ± 0.025 | 0.177 ± 0.051 | 0.227 ± 0.028 |
| 204628−7157.0 | 4.450 ± 0.059 | 1.866 ± 0.072 | 1.843 ± 0.071 | 1.520 ± 0.045 | 0.346 ± 0.019 | 2.456 ± 0.033 | 1.277 ± 0.019 | 12.118 ± 1.449 | 3.193 ± 0.390 |
| 205710+1939.0 | 2.573 ± 0.112 | 1.723 ± 0.220 | 0.617 ± 0.111 | 0.470 ± 0.138 | 1.253 ± 0.401 | 0.792 ± 0.042 | 1.230 ± 0.058 | 0.933 ± 0.206 | 1.992 ± 0.403 |
| 222257+1619.4 | 2.630 ± 0.021 | 1.863 ± 0.044 | 1.860 ± 0.045 | 0.493 ± 0.029 | 1.370 ± 0.105 | 0.818 ± 0.007 | 1.281 ± 0.012 | 0.915 ± 0.090 | 2.003 ± 0.185 |
| 233655+1548.1 | 4.182 ± 0.027 | 2.413 ± 0.046 | 2.044 ± 0.046 | 1.922 ± 0.023 | 0.492 ± 0.015 | 1.965 ± 0.018 | 1.305 ± 0.015 | 9.828 ± 1.170 | 2.620 ± 0.290 |
| 234535+2528.3 | 3.920 ± 0.016 | 2.409 ± 0.029 | 2.115 ± 0.028 | 1.720 ± 0.015 | 0.690 ± 0.013 | 2.120 ± 0.015 | 1.250 ± 0.024 | 9.673 ± 1.195 | 2.406 ± 0.333 |
| 234718−0805.2 | 3.254 ± 0.065 | 1.990 ± 0.117 | 1.663 ± 0.098 | 1.655 ± 0.070 | 0.336 ± 0.034 | 1.764 ± 0.036 | 0.898 ± 0.019 | 6.248 ± 0.917 | 1.025 ± 0.137 |

light-curve modelling technique and obtained $i(^\circ) = 63.50 \pm 0.67$, $f(M) = 1.704(50)\,\mathrm{M}_\odot$, $l_3 = 0.278 \pm 0.019$. The mass function $f(M)$ in all the three cases is quite similar. However, the absolute parameters determined using the ASAS light curve are different from those of Djurašević et al. (2006). This disagreement might be caused because of slightly noisy ASAS data and/or estimation of different values of third light contribution in the two analyses. Simultaneous multicolour photometry and the use of a spectral broadening function using high-resolution radial velocity curves can resolve the issue of accurate estimation of third light in the system. This will help in the determination of reliable parameters for this binary system.

**Table 6.** Physical parameters of 23 stars common to our sample as found in the literature.

| ID | $M_P/M_\odot$ | $M_S/M_\odot$ | $R_P/R_\odot$ | $R_S/R_\odot$ | $L_P/L_\odot$ | $L_S/L_\odot$ | References |
|---|---|---|---|---|---|---|---|
| 003628+2132.3 | 1.352 ± 0.057 | 0.183 ± 0.024 | 1.469 ± 0.021 | 0.617 ± 0.009 | 2.836 ± 0.081 | 0.493 ± 0.022 | Gazeas et al. (2005) |
| 012104+0736.3 | 1.682 ± 0.032 | 0.389 ± 0.017 | 1.753 ± 0.111 | 0.890 ± 0.002 | 3.760 ± 0.032 | 0.984 ± 0.008 | Gazeas et al. (2006) |
| 024952+0856.3 | 1.380 ± 0.004 | 0.430 ± 0.002 | 1.350 ± 0.002 | 0.820 ± 0.001 | 1.490 ± 0.007 | 1.580 ± 0.009 | Djurašević et al. (2006) |
| 030953−0653.6 | 1.450 ± 0.044 | 0.540 ± 0.017 | 1.450 ± 0.018 | 0.910 ± 0.011 | 2.440 ± 0.061 | 1.030 ± 0.025 | Qian et al. (2007b) |
| 034814+2218.9 | 1.230 ± 0.004 | 0.540 ± 0.002 | 1.140 ± 0.002 | 0.790 ± 0.002 | 1.330 ± 0.004 | 0.610 ± 0.002 | Yuan & Qian (2007) |
| 062605+2759.9 | 1.674 ± 0.048 | 0.283 ± 0.022 | 1.897 ± 0.018 | 0.837 ± 0.009 | 4.279 ± 0.090 | 1.090 ± 0.058 | Gazeas et al. (2005) |
| 064558−0017.5 | 1.390 ± 0.070 | 0.930 ± 0.060 | 1.440 ± 0.030 | 1.290 ± 0.030 | 2.780 ± 0.011 | 1.080 ± 0.005 | Gazeas, Liakos & Niarchos (2009) |
| 071058−0352.8 | 1.528 ± 0.020 | 1.482 ± 0.020 | 1.738 ± 0.006 | 1.592 ± 0.007 | 8.446 ± 0.011 | 7.551 ± 0.012 | Zola et al. (2004) |
| 084002+1900.0 | 1.350 ± 0.020 | 0.610 ± 0.010 | 1.270 ± 0.040 | 0.890 ± 0.030 | 2.130 ± 0.110 | 1.260 ± 0.070 | Zhang, Deng & Lu (2009) |
| 100234+1702.8 | 1.742 ± 0.047 | 0.586 ± 0.027 | 1.689 ± 0.015 | 1.004 ± 0.009 | 6.926 ± 0.043 | 2.073 ± 0.020 | Gazeas et al. (2006) |
| 105030−0241.7 | 1.423 ± 0.016 | 0.449 ± 0.009 | 1.497 ± 0.008 | 0.864 ± 0.006 | 2.174 ± 0.022 | 0.832 ± 0.008 | Gazeas et al. (2006) |
| 110505+0509.1 | 1.470 ± 0.000 | 0.440 ± 0.000 | 1.490 ± 0.000 | 0.870 ± 0.000 | 2.846 ± 0.000 | 1.003 ± 0.000 | Qian et al. (2007a) |
| 134607+0506.9 | 1.284 ± 0.015 | 1.046 ± 0.013 | 1.223 ± 0.005 | 1.107 ± 0.004 | 1.720 ± 0.002 | 1.500 ± 0.001 | Zola et al. (2005) |
| 141726+1234.1 | 0.980 ± 0.004 | 0.420 ± 0.002 | 1.080 ± 0.002 | 0.740 ± 0.002 | 1.100 ± 0.036 | 0.360 ± 0.006 | Rainger, Bell & Hilditch (1990) |
| 141937+0553.8 | 1.730 ± 0.024 | 0.850 ± 0.017 | 1.717 ± 0.008 | 1.246 ± 0.007 | 5.905 ± 0.055 | 3.155 ± 0.060 | Gazeas et al. (2005) |
| 152243+1615.7 | 1.109 ± 0.038 | 0.192 ± 0.008 | 1.148 ± 0.007 | 0.507 ± 0.006 | 1.480 ± 0.010 | 0.340 ± 0.020 | Zola et al. (2005) |
| 153152−1541.1 | 1.060 ± 0.060 | 0.350 ± 0.030 | 1.170 ± 0.050 | 0.720 ± 0.030 | 1.360 ± 0.190 | 0.590 ± 0.050 | Szalai et al. (2007) |
| 165717+1059.8 | 1.191 ± 0.012 | 0.288 ± 0.009 | 1.392 ± 0.018 | 0.689 ± 0.009 | 1.782 ± 0.030 | 0.468 ± 0.011 | Gazeas et al. (2006) |
| 171358+1621.0 | 1.860 ± 0.010 | 0.480 ± 0.010 | 1.660 ± 0.010 | 0.960 ± 0.010 | 4.430 ± 0.010 | 0.970 ± 0.010 | Samadi et al. (2010) |
| 180921+0909.1 | 1.572 ± 0.031 | 0.462 ± 0.042 | 1.528 ± 0.010 | 0.874 ± 0.006 | 3.148 ± 0.020 | 1.097 ± 0.010 | Gazeas et al. (2006) |
| 193524+0550.3 | 1.377 ± 0.036 | 0.498 ± 0.022 | 1.314 ± 0.012 | 0.808 ± 0.008 | 1.796 ± 0.033 | 0.777 ± 0.041 | Gazeas et al. (2006) |
| 194813+0918.5 | 1.040 ± 0.002 | 0.880 ± 0.002 | 1.390 ± 0.002 | 1.290 ± 0.002 | 1.910 ± 0.039 | 1.560 ± 0.032 | Hrivnak (1989) |
| 222257+1619.4 | 1.420 ± 0.040 | 0.530 ± 0.020 | 1.290 ± 0.040 | 0.830 ± 0.020 | 1.860 ± 0.080 | 0.940 ± 0.060 | Kalomeni et al. (2007) |

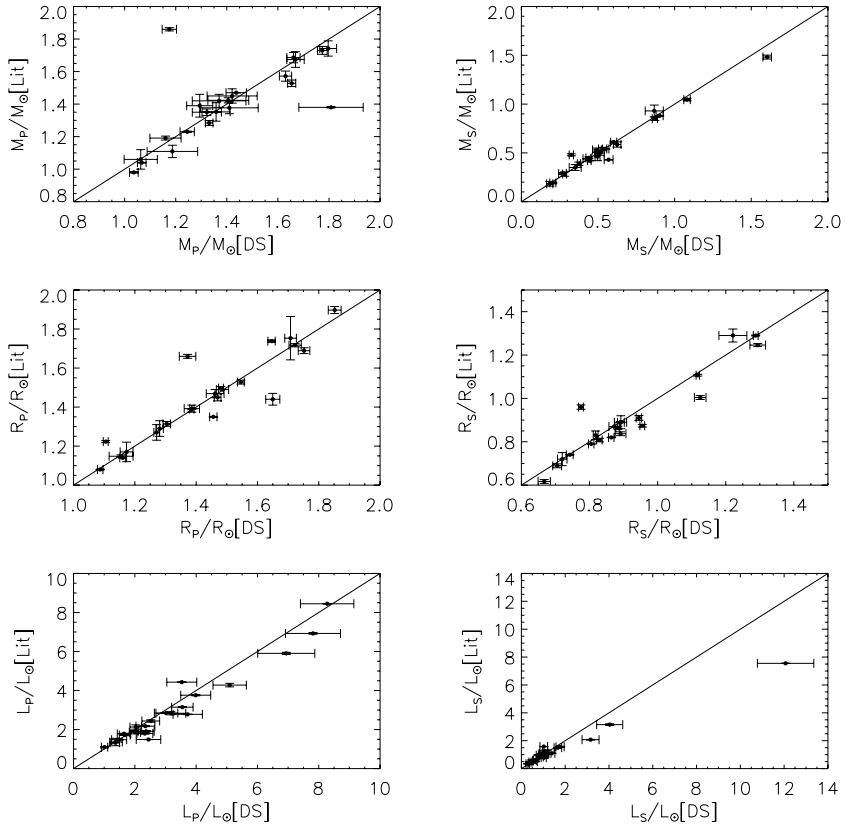


**Figure 9.** The comparison of primary and secondary component parameters of 23 stars in our sample common to the literature. The parameters determined by us are plotted on the *x*-axis while those in the literature are plotted on the *y*-axis. The clustering of most of the data points along a line (solid) indicates a positive linear correlation.

**Table 7.** Parameters for the components of EE Cet and comparison with previous study.

| Parameter | Djurašević et al. (2006) | This study |
|---|---|---|
| $q$(fixed) | 0.315 | 0.315 |
| $M_P$ ($M_\odot$) | 1.37(4) | 1.808(126) |
| $M_S$ ($M_\odot$) | 0.43(2) | 0.569(29) |
| $R_P$ ($R_\odot$) | 1.35(2) | 1.456(12) |
| $R_S$ ($R_\odot$) | 0.82(1) | 0.864(8) |
| $L_P$ ($L_\odot$) | 1.58(9) | 2.445(400) |
| $L_S$ ($L_\odot$) | 1.49(7) | 1.020(173) |

**Table 8.** Parameters for the components of V753 Mon and comparison with previous study.

| Parameter | Zola et al. (2004) | This study |
|---|---|---|
| $q$(fixed) | 0.971 | 0.970 |
| $M_P$ ($M_\odot$) | 1.528(20) | 1.654(16) |
| $M_S$ ($M_\odot$) | 1.482(20) | 1.604(28) |
| $R_P$ ($R_\odot$) | 1.738(7) | 1.646(12) |
| $R_S$ ($R_\odot$) | 1.592(6) | 1.935(12) |
| $L_P$ ($L_\odot$) | 8.446(68) | 8.274(871) |
| $L_S$ ($L_\odot$) | 7.551(112) | 12.067(1.288) |

### 6.3 ASAS 071058−0352.8 = V753 Mon

V753 Mon is a new discovery of the *Hipparcos* mission. The radial velocity measurements of the star were obtained by Rucinski et al. (2000) who found a spectroscopic mass ratio of $q_{sp} = 0.970$. The star was classified as a W UMa binary of subtype W with spectral type A8V by the authors. The recent photometric analysis of the star by Zola et al. (2004) yields the following parameters of the binary: $i(^\circ) = 75.30 \pm 0.13$, $\Delta T \sim 120$ K, using a semidetached configuration with the slightly less massive component filling its Roche lobe. Our photometric analysis of the ASAS light curve also shows that the configuration of the system is not a contact one. The star is marked with the serial number '20' in Fig. 5 and lies above the contact envelope. We have also found a semidetached configuration with the secondary star filling its Roche lobe from the ASAS light-curve modelling. We found $i(^\circ) = 74.85 \pm 0.07$, $\Delta T \sim 104$ K. We now compare our mass function determination with Zola et al. (2004) and Rucinski et al. (2000). The physical parameters obtained by Zola et al. (2004) and those determined by us are listed in Table 8. The mass function estimated from Zola et al. (2004) is 2.724 $M_\odot$, following equation (5). On the other hand, the mass function obtained from the ASAS light curve is $f(M) = 2.930(34)\,M_\odot$ and is identical to the spectroscopic estimate 2.93(6) $M_\odot$ of Rucinski et al. (2000). However, the mass function derived from Zola et al. (2004) is quite different from both the spectroscopic estimate of Rucinski et al. (2000) and that determined by us. Therefore the parameters determined by Zola et al. (2004) need to re-examined.

### 6.4 ASAS 171358+1621.0 = AK Her

AK Her is the brighter component in the visual binary ADS 10408. The companion, located at a separation of 4.2 arcsec, is 3.5 mag fainter than AK Her at its maximum light (Pribulla et al. 2006). The star has been the subject of numerous studies (Samadi et al. 2010, and references therein). These suggest that the system has a variable light curve and a variable period. Analysis of the updated *O–C* curves revealed evidence of continuously changing period with cycle length between 57 and 97 yr (Samadi et al. 2010). Using the spectroscopic mass ratio of 0.26 from Sanford (1934), Samadi et al. (2010) derived $i(^\circ) = 83.88 \pm 0.27$ and the parameters as listed in Table 9. Using the spectroscopic radial velocity measurements, Pribulla et al. (2006) obtained $K_1 = 70.52 \pm 1.12\,\mathrm{km\,s^{-1}}$, $K_2 = 254.40 \pm 2.27\,\mathrm{km\,s^{-1}}$. Pribulla et al. (2006) quoted $f(M) = 1.598(29)$, while the correct value should be 1.502(29), which can be calculated from equation (5). From Samadi et al. (2010), one can calculate the value of the mass function $f(M) = (M_1 + M_2)\sin^3(i) = 2.300\,M_\odot$. This value is quite different from the spectroscopic estimate 1.502(29). Hence, the parameters determined by Samadi et al. (2010) may not be reliable. We have analysed the ASAS light curve of AK Her using the spectroscopic mass ratio $q_{sp} = 0.277$, considering A-type configuration and a spectral type F4V (Pribulla et al. 2006). Using the ASAS data, we calculated the mass function for the system as 1.500(37) $M_\odot$, which is nearly identical to the spectroscopic estimate of Pribulla et al. (2006).

**Table 9.** Parameters for the components of AK Her and comparison with previous study.

| Parameter | Samadi et al. (2010) | This study |
|---|---|---|
| $q$(fixed) | 0.26 | 0.277 |
| $M_P$ ($M_\odot$) | 1.86(1) | 1.175(28) |
| $M_S$ ($M_\odot$) | 0.48(1) | 0.326(14) |
| $R_P$ ($R_\odot$) | 1.66(1) | 1.372(27) |
| $R_S$ ($R_\odot$) | 0.96(1) | 0.775(7) |
| $L_P$ ($L_\odot$) | 4.43(1) | 3.531(489) |
| $L_S$ ($L_\odot$) | 0.97(1) | 0.760(82) |

## 7 VARIOUS RELATIONS OF CONTACT BINARIES

### 7.1 Period–mass relation for contact binaries

Various studies suggest that there exists a period–mass relation for contact binaries (Qian 2003; Gazeas & Niarchos 2006; Gazeas & Stępień 2008). Qian (2003) noted that the mass of the primary component (more massive) increases linearly with increasing period. Gazeas & Niarchos (2006) also noted the same and found that the mass of the secondary component (less massive) is nearly period-independent and varies between 0 and 1 $M_\odot$. From a sample of 112 binaries (52 W-type and 60 A-type), Gazeas & Niarchos (2006) derived the following relations between the masses of the components and the orbital period ($P$):

$$\log M_P = (0.755 \pm 0.059)\log P + (0.416 \pm 0.024), \quad (6)$$

$$\log M_S = (0.352 \pm 0.166)\log P - (0.262 \pm 0.067). \quad (7)$$

In Fig. 10, we have plotted $\log M_P$ versus $\log P$ and $\log M_S$ versus $\log P$ for the 54 contact binaries in our sample. Also overplotted are the solid lines from the relations of equations (6) and (7) in this paper obtained by Gazeas & Niarchos (2006). It can be seen that the masses of the primary components, in general, obey the period–mass relation defined by equation (6), whereas the secondary components do not seem to obey any strict period–mass relation of equation (7) as derived by Gazeas & Niarchos (2006).

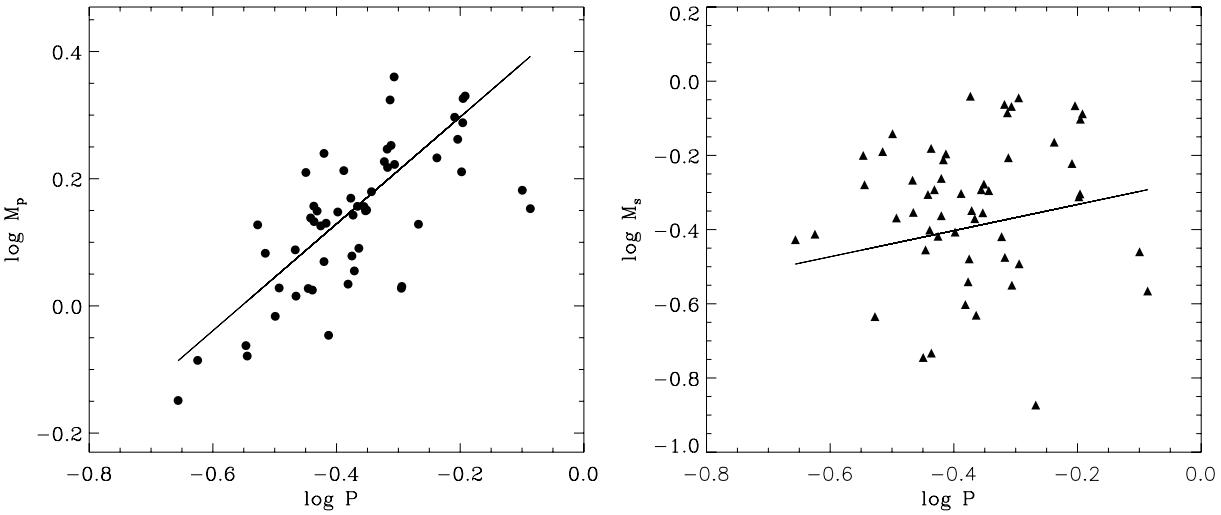


**Figure 10.** The left- and right-hand panels show the masses of the primary and secondary components of 54 contact binaries in our sample on the log $P$–log $M_{\rm P}$ and log $P$–log $M_{\rm S}$ plane. Solid lines in the two plots are the linear fits from equations (6) and (7), as derived by Gazeas & Niarchos (2006).

### 7.2 Period–colour relations of contact binaries

Contact binaries obey a well-defined period–colour relation. This relation plays a special role in the study of their properties (Rucinski 1997b, 2000). The period–colour relations of equal mass marginal contact binaries over a wide range of age and metallicity were studied by Rubenstein (2001). Rucinski (2000) derived the shapes of short period blue envelopes (SPBEs) for disc systems by the following two power-law relations:

$$(B - V) = 0.04P^{-2.25} \tag{8}$$

and

$$(V - I) = 0.053P^{-2.1}. \tag{9}$$

Here we examine the period ($P$)–infrared colour ($J - K$) relation of 141 contact binaries. The relation that we derive here is just a power-law fit to the data in the $P$–($J - K$) plane, whereas Rucinski's SPBE is rather a limit for colour and period of stars. Because of the advantage of ($J - K$) colour not affected by the interstellar extinction and uncertain reddening corrections as compared to the ($B - V$) colour, the period–colour relation using the infrared colour ($J - K$) will be helpful for larger data bases, where the period can be determined easily with greater accuracy. In the present study, the infrared colour is obtained from the *JHK* magnitudes in the 2MASS point source catalogue (Cutri et al. 2003). To increase the number of samples to derive the $P$–($J - K$) relation, we took 129 W UMa contact binaries from Bilir et al. (2005). For one star, GZ And, in the sample, there is no reliable *JHK* magnitude available in the 2MASS catalogue. On the other hand, two stars in the Bilir's sample, V753 Mon and HT Vir, turned out to be semidetached binaries in our analysis. Therefore, these three stars were rejected for deriving the period–infrared colour relation of contact binaries. Hence, out of 129 stars in the Bilir's sample, we have selected 126 stars for the analysis. On the other hand, among 126 stars, 39 of them are common to our sample of 54 contact binaries. Therefore, the total sample used for deriving the ($J - K$) versus $P$ relation for contact binaries is 141. Fig. 11 shows the period–colour ($J - K$) for all 141 contact binaries in the total sample. From the figure, it is very clear that contact binaries definitely obey a tight period ($P$)–colour ($J - K$) relation. From the 141 contact binaries,

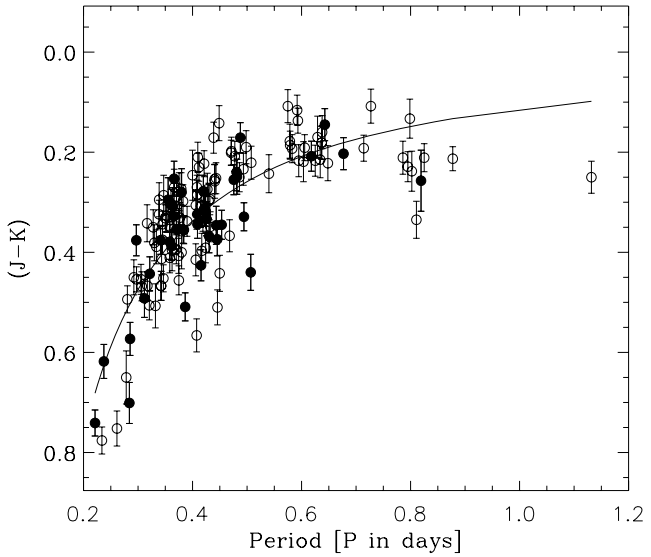


**Figure 11.** Period ($P$)–colour ($J - K$) relation of 141 contact binaries obtained from the combined data of 54 ASAS contact binaries and data from Bilir et al. (2005). The 39 stars common to our sample are shown by filled circles. The solid line is the power-law fit to the data of these contact binaries as given in equation (10).

we derived the following relation:

$$(J - K) = (0.11 \pm 0.01)P^{-1.19\pm0.08}. \tag{10}$$

The fit to this derived relation is shown by the solid line in Fig. 11. Derivation of such an empirical period–colour relation of contact binaries using accurate infrared colours will be very useful to display the properties of contact binaries discovered in large photometric surveys. However, the derivation of precise period–colour relations of contact binaries needs highly accurate age and metallicity estimations (Rubenstein 2001).

### 7.3 *M–R* and *M–L* diagrams

Fig. 12 shows the location of the components of detached binaries on the theoretical mass–radius (*M–R*) and mass–luminosity (*M–L*) diagrams along with the 0.06, 0.50, 2.0, 5.0 and 10 Gyr

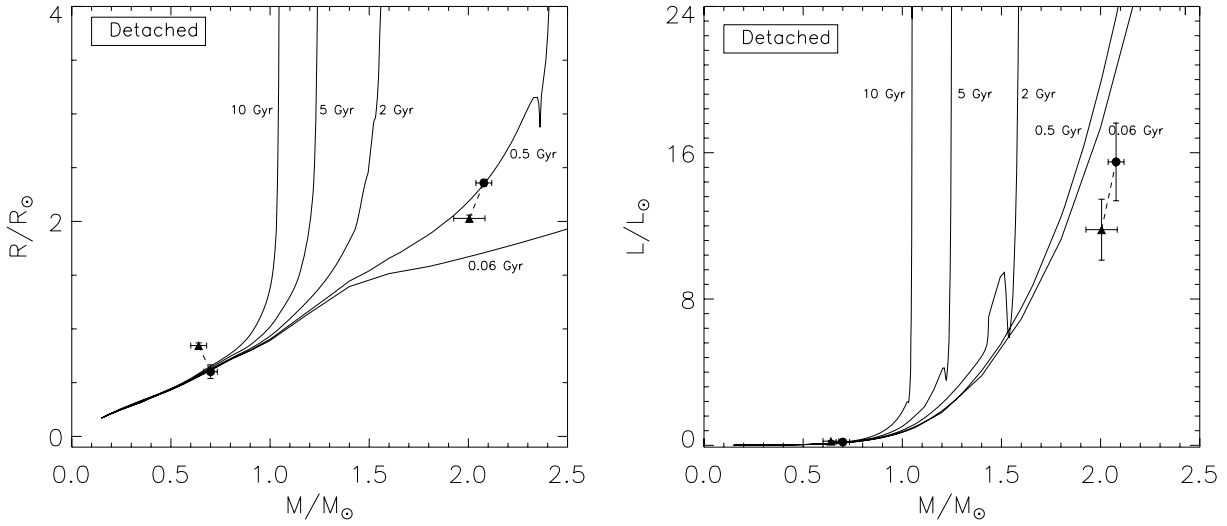


**Figure 12.** Location of the components of detached binaries on the theoretical mass–luminosity (*M–L*) and mass–radius (*M–R*) diagrams along with the 0.06, 0.50, 2.0, 5.0 and 10 Gyr theoretical isochrones from Girardi et al. (2000) for Population I stars with solar composition ($X$, $Y$, $Z$) = 0.708, 0.273, 0.019. Each isochrone is plotted as a solid line and labelled with its corresponding age. Primary (more massive) components are plotted with filled circles, and secondary components (less massive) with filled upper triangles. The components of the same pair are connected with dotted lines.

theoretical isochrones from Girardi et al. (2000) for the Population I stars with the solar composition ($X$, $Y$, $Z$) = 0.708, 0.273, 0.019. Each isochrone is plotted as a solid line and labelled with its corresponding age. Primary (more massive) components are plotted with filled circles and secondary components (less massive) with filled upper triangles. The components of the same pair are connected with dotted lines. We have not tried to estimate the ages of the components of contact binaries. The ages of the primary components can be determined by interpolation from the isochrone fitting. As in general, to an approximation, they obey a normal mass–radius relations for main-sequence stars. On the other hand, the secondary components of contact binaries are always overluminous and oversized for their mass and do not obey the normal main-sequence mass–radius relations. Hence, it is difficult to calculate their age from the main-sequence isochrone fitting. However, the peculiar evolutionary status of the contact binaries due to the effect of a vast amount of mass transfer is also seen. The result of such an effect is the underluminous and undersized primary component and overluminous and oversized secondary component (Zhang et al. 2009). In fact, it would be wrong to make comparisons between the empirical data on mass and absolute dimensions for such systems and the theoretical stellar evolution of single stars alone. The stellar evolution theory is very much complicated which takes into account the mass loss, the existence of the upper limit of the volume of a star and to allow for changes in orbital period and sizes due to the effect of mass transfer for semidetached and contact binaries, and is beyond the scope of this present work. For the two detached binaries in our sample, 203113+0513.2 appears to have an age $\geq$10 Gyr, whereas 084108−3212.1 has an age $\leq$0.5 Gyr from the *M–R* diagram. However, determination of their accurate ages needs parameter estimations from highly precise light curves.

## 8 SUMMARY AND CONCLUSIONS

We have explored the ASAS data base to study eclipsing binaries. We have presented a detailed analysis of the light curves of 62 eclipsing binaries monitored by the ASAS project which have precise radial velocity measurements in the literature.

We updated the ASAS periods using the ME method and classified the stars based on their light-curve shapes. With the improved ASAS periods, we obtained significant improvement in the light-curve shapes. For preliminary classification, we have used cosine decomposition of the light curves into the Fourier coefficients, where contact, semidetached and detached configurations can be distinguished in the $a_2$–$a_4$ plane. Further, using the Roche lobe geometry, we found that the sample contains 54 contact, six semidetached and two detached binaries. The physical parameters of all 62 binaries were calculated using the WD light-curve modelling technique. Spectroscopic mass ratios of these binaries available in the literature were used for their modelling. Out of 62 stars in the sample, light-curve analysis of 39 stars is presented here for the first time using combined photometric and spectroscopic data. For the majority of the remaining 23 stars, the determination of parameters is found to be consistent with the earlier values obtained in the literature. Thus, ASAS-like data bases can, in general, be used for parameter determinations of newly discovered eclipsing binaries for statistical analysis. An ASAS-like data base opens a new avenue to study the parameters of eclipsing binaries in large numbers. Availability of data of a huge number of eclipsing binaries in these data bases will facilitate measurements of their geometrical and physical parameters, if precise mass ratios are determined from spectroscopy. Spectroscopic measurements combined with the photometry from large data bases will provide an opportunity to understand the origin and evolution of binaries accurately and will resolve the longstanding issues of formation and evolution of contact binaries. It is therefore an urgent need to come up with projects which will be solely devoted to radial velocity measurements of eclipsing binaries discovered in various automated photometric surveys and hence enhance our knowledge about the formation, structure and evolution of stars.

## ACKNOWLEDGMENTS

SD thanks CSIR, Government of India, for a Senior Research Fellowship. The authors acknowledge helpful discussions with Philippe Prugniel and Biman Jyoti Medhi, and thank the anonymous

referee for many insightful comments and suggestions which have led to the substantial improvement of the paper. The authors thank Alceste Z. Bonanos for a discussion on error estimation via e-mail. The use of the SIMBAD and ADS data bases is gratefully acknowledged. This publication makes use of data products from the Two Micron All Sky Survey, which is a joint project of the University of Massachusetts and the Infrared Processing and Analysis Center/California Institute of Technology, funded by the National Aeronautics and Space Administration and the National Science Foundation.

## REFERENCES

Bilir S., Karataş Y., Demircan O., Eker Z., 2005, MNRAS, 357, 497
Bonanos A. Z., 2009, ApJ, 691, 407
Bonanos A. Z. et al., 2006, ApJ, 652, 313
Cincotta P. M., Mendez M., Nunez J. A., 1995, ApJ, 449, 231
Cox A. N., 2000, Allen's astrophysical quantities, 4th edn. AIP Press (Springer), New York
Csizmadia S., Klagyivik P., 2004, A&A, 426, 1001
Cutri R. M. et al., 2003, 2MASS All Sky Catalog of point sources. NASA/IPAC Infrared Science Archive, http://irsa.ipac.caltech.edu/applications/Gator/
Deb S., Tiwari S. K., Singh H. P., Seshadri T. R., Chaubey U. S., 2009, Bull. Astron. Soc. India, 37, 109
Derekas A., Kiss L. L., Bedding T. R., 2007, ApJ, 663, 249
Djurašević G., Dimitrov D., Arbutina B., Albayrak B., Selam S. O., Atanacković-Vukmanović O., 2006, Publ. Astron. Soc. Aust., 23, 154
Duerbeck H. W., Rucinski S. M., 2007, AJ, 133, 169
Gazeas K. D., Niarchos P. G., 2006, MNRAS, 370, L29
Gazeas K., Stępień K., 2008, MNRAS, 390, 1577
Gazeas K. D. et al., 2005, Acta Astron., 55, 123
Gazeas K. D., Niarchos P. G., Zola S., Kreiner J. M., Rucinski S. M., 2006, Acta Astron., 56, 127
Gazeas K., Liakos A., Niarchos P., 2009, arXiv:0910.2911
Girardi L., Bressan A., Bertelli G., Chiosi C., 2000, A&AS, 141, 371
Hełminiak K. G., Konacki M., Ratajczak M., Muterspaugh M. W., 2009, MNRAS, 400, 969
Hrivnak B. J., 1989, ApJ, 340, 458
Kalomeni B., Yakut K., Keskin V., Değirmenci Ö. L., Ulaş B., Köse O., 2007, AJ, 134, 642
Kaluzny J., 1986, PASP, 98, 662
Kang Y. W., Oh K., Kim C., Hwang C., Kim H., Lee W., 2002, MNRAS, 331, 707
Lu W., Rucinski S. M., 1999, AJ, 118, 515
Lu W., Rucinski S. M., Ogłoza W., 2001, AJ, 122, 402
Lucy L. B., Wilson R. E., 1979, ApJ, 231, 502
Maceroni C., van't Veer F., 1993, A&A, 277, 515
Maceroni C., Vilhu O., van't Veer F., van Hamme W., 1994, A&A, 288, 529
O'Connell D. J. K., 1951, Publ. Riverview College Obser., 2, 85
Paczynski B., 1997, in Livio M., ed., The Extragalactic Distance Scale. Cambridge Univ. Press, Cambridge, p. 273
Paczyński B., Szczygieł D. M., Pilecki B., Pojmański G., 2006, MNRAS, 368, 1311
Parihar P., Messina S., Bama P., Medhi B. J., Muneer S., Velu C., Ahmad A., 2009, MNRAS, 395, 593
Percy J. R., 2007, Understanding variable stars. Cambridge Univ. Press, Cambridge
Perryman M. A. C., ESA eds, 1997, The HIPPARCOS and TYCHO catalogues. Astrometric and photometric star catalogues derived from the ESA HIPPARCOS Space Astrometry Mission, Vol. 1200. ESA Publications Division, Noordwijk
Pojmanski G., 1997, Acta Astron., 47, 467
Pojmanski G., 1998, Acta Astron., 48, 35
Pojmanski G., 2002, Acta Astron., 52, 397
Pribulla T. et al., 2006, AJ, 132, 769
Pribulla T., Rucinski S. M., Conidis G., DeBond H., Thomson J. R., Gazeas K., Ogłoza W., 2007, AJ, 133, 1977
Pribulla T. et al., 2009a, AJ, 137, 3646
Pribulla T. et al., 2009b, AJ, 137, 3655
Prša A., Zwitter T., 2005, ApJ, 628, 426
Pych W. et al., 2004, AJ, 127, 1712
Qian S., 2003, MNRAS, 342, 1260
Qian S., Xiang F., Zhu L., Dai Z., He J., Yuan J., 2007a, AJ, 133, 357
Qian S., Yuan J., Xiang F., Soonthornthum B., Zhu L., He J., 2007b, AJ, 134, 1769
Rainger P. P., Bell S. A., Hilditch R. W., 1990, MNRAS, 246, 47
Rubenstein E. P., 2001, AJ, 121, 3219
Rucinski S. M., 1993, PASP, 105, 1433
Rucinski S. M., 1997a, AJ, 113, 1112
Rucinski S. M., 1997b, AJ, 113, 407
Rucinski S. M., 2000, AJ, 120, 319
Rucinski S. M., 2001, AJ, 122, 1007
Rucinski S. M., 2002, AJ, 124, 1746
Rucinski S. M., Duerbeck H. W., 1997, PASP, 109, 1340
Rucinski S. M., Duerbeck H. W., 2006, AJ, 132, 1539
Rucinski S. M., Lu W., 1999, AJ, 118, 2451
Rucinski S. M., Lu W., Mochnacki S. W., 2000, AJ, 120, 1133
Rucinski S. M., Lu W., Mochnacki S. W., Ogłoza W., Stachowski G., 2001, AJ, 122, 1974
Rucinski S. M., Lu W., Capobianco C. C., Mochnacki S. W., Blake R. M., Thomson J. R., Ogłoza W., Stachowski G., 2002, AJ, 124, 1738
Rucinski S. M. et al., 2003, AJ, 125, 3258
Rucinski S. M. et al., 2005, AJ, 130, 767
Rucinski S. M. et al., 2008, AJ, 136, 586
Samadi A., Jassur D. M. Z., Nassiri S., Gozaliasl G., Kermani M. H., Zareie A., 2010, New Astron., 15, 339
Sanford R. F., 1934, ApJ, 79, 89
Shu F. H., 1982, The Physical Universe. University Science Books, Mill Valley, CA
Stellingwerf R. F., 1978, ApJ, 224, 953
Szalai T., Kiss L. L., Mészáros S., Vinkó J., Csizmadia S., 2007, A&A, 465, 943
Tas G., Evren S., 2006, Inf. Bull. Variable Stars, 5687, 1
van Hamme W., 1993, AJ, 106, 2096
Vilardell F., Ribas I., Jordi C., Fitzpatrick E. L., Guinan E. F., 2010, A&A, 509, A70
Wilson R. E., 1979, ApJ, 234, 1054
Wilson R. E., 1990, ApJ, 356, 613
Wilson R. E., Devinney E. J., 1971, ApJ, 166, 605
Yuan J., Qian S., 2007, ApJ, 669, L93
Zhang X. B., Deng L., Lu P., 2009, AJ, 138, 680
Zola S. et al., 2004, Acta Astron., 54, 299
Zola S. et al., 2005, Acta Astron., 55, 389

## SUPPORTING INFORMATION

Additional Supporting Information may be found in the online version of this article:

**Table 3.** The Fourier parameters of the ASAS eclipsing binaries used for the analysis.

Please note: Wiley-Blackwell are not responsible for the content or functionality of any supporting materials supplied by the authors. Any queries (other than missing material) should be directed to the corresponding author for the article.

This paper has been typeset from a TEX/LATEX file prepared by the author.